were resolved by using 10% Bis-Tris Criterion XT Precast gels (Bio-Rad Laboratories, Hercules, CA, USA), transferred to PVDF membranes or stained with CBB. For 2-DE, IEF was carried out using the PROTEAN IEF cell (Bio-Rad Laboratories) according to the manufacturer's instructions. Extracted proteins were reconstituted in a rehydration buffer (7 M urea, 2 M thiourea, 4% CHAPS, 2 mM tributyl phosphine (TBP), 0.0002% bromophenol blue (BPB), 0.2% bio-lyte ampholyte 3-10) and applied to ReadyStrip IPG strips (11 cm, pH 3–10). IEF was run for 45 000 Vh, and 2-DE was carried out using 10% Bis-Tris Criterion XT Precast gels. The gels were then stained with the Silver Stain MS Kit (Wako Pure Chemical Industries, Osaka, Japan) or used for protein transfer to PVDF membranes.

Western blotting. After blocking with 5% skim milk, the PVDF membranes were incubated with serum at a 1:100 dilution or rabbit anti-enolase antibody (Santa Cruz Biotechnology, Santa Cruz, CA, USA) at a 1:1500 dilution. The membranes were then incubated with sheep anti-human IgG or donkey anti-rabbit IgG (Amersham Biosciences UK, Buckinghamshire, UK). Membranes incubated with sheep anti-human IgG only were used as negative controls. Finally, the signals were visualized with an enhanced chemiluminescence reaction system (Perkin Elmer Life Sciences, Boston, MA, USA).

Identification of protein bands or spots. Protein bands on gels stained with CBB or protein spots on gels stained with silver, which corresponded to positive bands or spots on western blot membranes, were excised from the gel and digested with trypsin (Promega, Madison, WI, USA) according to published procedures.[18] For protein bands, the LC-MS/MS analysis was carried out using an LCQ ion trap mass spectrometer (ThermoElectron, San Jose, CA, USA) coupled on-line with Magic 2002 capillary high-performance liquid chromatography (Michrom BioResources, Auburn, CA, USA). For protein spots, all PMF spectra were obtained by using an ultraflex TOF/TOF MALDI-TOF mass spectrometer (Bruker Daltonics, Bremen, Germany). MS/MS or PMF data were then searched with Mascot software (Matrix Science, London, UK) against the NCBInr or swiss-prot databases. Protein database searching was carried out with following parameters for PMF: *Homo sapiens*, maximum of one missed, cleavage by trypsin, monoisotopic mass value, charge state of 1+, allowing a mass tolerance of 100 p.p.m., and carbamidomethyl modification of cysteine.

Preparation of recombinant protein. To prepare recombinant proteins, the human full-length α-enolase complementary DNA (1–434 a.a.) was amplified by PCR from the Hep3B cell line cDNA library using the primers: sense 5′-GTGGCTAGAAGT-TCACCATG-3′, antisense 5′-TTACTTGGCCAAGGGGTTTC-3′. To map the autoepitope on α-enolase, three cDNA fragments that encode C-terminal deletion mutant proteins (α-Eno1, α-Eno2, α-Eno3) were similarly amplified. The nucleotide sequences of the primers for PCR were: α-Eno1 (1–334 a.a.) sense 5′-TGTCTATTCTCAAGATCCATGCC-3′, antisense 5′-TTACTCGTTCACGGCCTTGGC-3′; α-Eno2 (1–234 a.a.), sense 5′-TGTCTATTCTCAAGATCCATGCC-3′, antisense 5′-TTAAGCTTTCCCAATAGCAGTC-3′; and α-Eno3 (1–134 a.a.) sense 5′-TGTCTATTCTCAAGATCCATGCC-3′, antisense 5′-TTAGATGTGGCGGTACAGGGG-3′. These cDNA fragments were then subcloned into the pET-28a(+) vector (Novagen, Madison, WI, USA), resulting in expression of α-enolase or its fragments with a 6 × His tag. Recombinant proteins were produced in *Escherischia coli* BL21-CodonPlus (DE3)-RIL cells (Stratagene, La Jolla, CA, USA) and purified by affinity chromatography using Ni-NTA resin (QIAGEN, Tokyo, Japan). Recombinant human full-length or C-terminal deletion mutant α-enolase, rabbit β-enolase (Sigma, St Louis, MO, USA) and human γ-enolase (Calbiochem) were subjected to sodium dodecylsulfate–polyacrylamide gel electrophoresis, using a 4–20% precast gel, then stained with CBB or transferred to PVDF membrane and probed with anti-enolase antibody, anti-6 × His monoclonal antibody or sera as described above.

Flow cytometry. Human lung adenocarcinoma cell line A549 was maintained in RPMI-1640 medium supplemented with 10% heat-inactivated fetal bovine serum, 100 U/mL penicillin and 100 μg/mL streptomycin. Cells (10^6) were incubated with rabbit anti-enolase antibody at a 1:100 dilution and labeled with fluorescein isothiocyanate-conjugated goat anti-rabbit immunoglobulin (BD Biosciences, San Jose, CA, USA). Normal rabbit IgG was used as a control. Stained cells were analyzed using a FACS Canto cytometer (Becton-Dickinson, Mountain View, CA, USA) and the results were analyzed using FlowJo software (Tree Star, Stanford, CA, USA).

ELISA. To assess the potential of these autoantibodies as a diagnostic marker, their frequencies in the sera were determined by means of ELISA using recombinant human full-length α-enolase protein. The ELISA was carried out as published elsewhere, with modifications.[19] Briefly, each well of a Microtiter plate (MaxiSorp; Nunc A/S, Roskilde, Denmark) was coated with 1 μg of recombinant human full-length α-enolase. After blocking with 1% bovine serum albumin, all wells were incubated with human serum at a 1:500 dilution at room temperature for 1 h. To reduce the background level originating from the non-specific reactivity of sera with bacterial proteins, the sera were diluted and incubated with 100 μg/mL *E. coli* BL21-CodonPlus (DE3)-RIL cell lysate for 2 h at room temperature before incubation with coated recombinant human α-enolase. The antigen–antibody complexes were detected with 1:5000-diluted HRP-conjugate sheep anti-human IgG with TMB (Dako, Carpinteria, CA, USA) as the substrate. OD was read at 450 nm. The antibody titer was expressed by using arbitrary binding units calculated according to the formula:

$$\text{binding units of sample} = (OD_{\text{sample}}/[\text{Mean } OD_{\text{healthy control sera}} + 3\ SD_{\text{healthy control sera}}]) \times 100.$$

Based on this formula, 100 binding units was used as the cut-off point.

IHC staining. After deparaffinization, tissue sections were treated with 100% cold methanol containing freshly prepared 0.3% hydrogen peroxide for 30 min, blocked in 10% normal goat serum for 20 min and incubated with rabbit anti-enolase antibody (Santa Cruz Biotechnology) at a 1:250 dilution overnight. Incubation of parallel sections omitting the first antibody was done to generate negative controls. Staining of sections was completed with a biotin-conjugated secondary antibody, HRP-conjugated streptavidin and diaminobenzidine.

Statistical analysis. Significant differences between groups were assessed with the χ^2-test and Fisher's exact test. $P < 0.05$ was considered significant.

Results

Detection of autoantigens associated with NSCLC by 1-DE western blotting and LC-MS/MS. In order to screen for autoantibodies against cancer cells in patients with NSCLC, proteins extracted from a given patient's tumor tissue were subjected to 1-DE, transferred to membranes, and incubated with sera from the same patient or from healthy control subjects. Membranes incubated with only the secondary antibody were used as negative controls. An approximately 47-kDa band was recognized only by a subset of NSCLC patient sera, whereas no such reaction was observed with healthy control sera or negative controls (Fig. 1a). To identify this 47-kDa protein, the corresponding band on the gel stained with CBB was digested and analyzed using LC-MS/MS. The eight proteins, including α-enolase and elongation factor 1-α 1, which were identified by database searching through Mascot software, are listed in Table 1. Many of these proteins

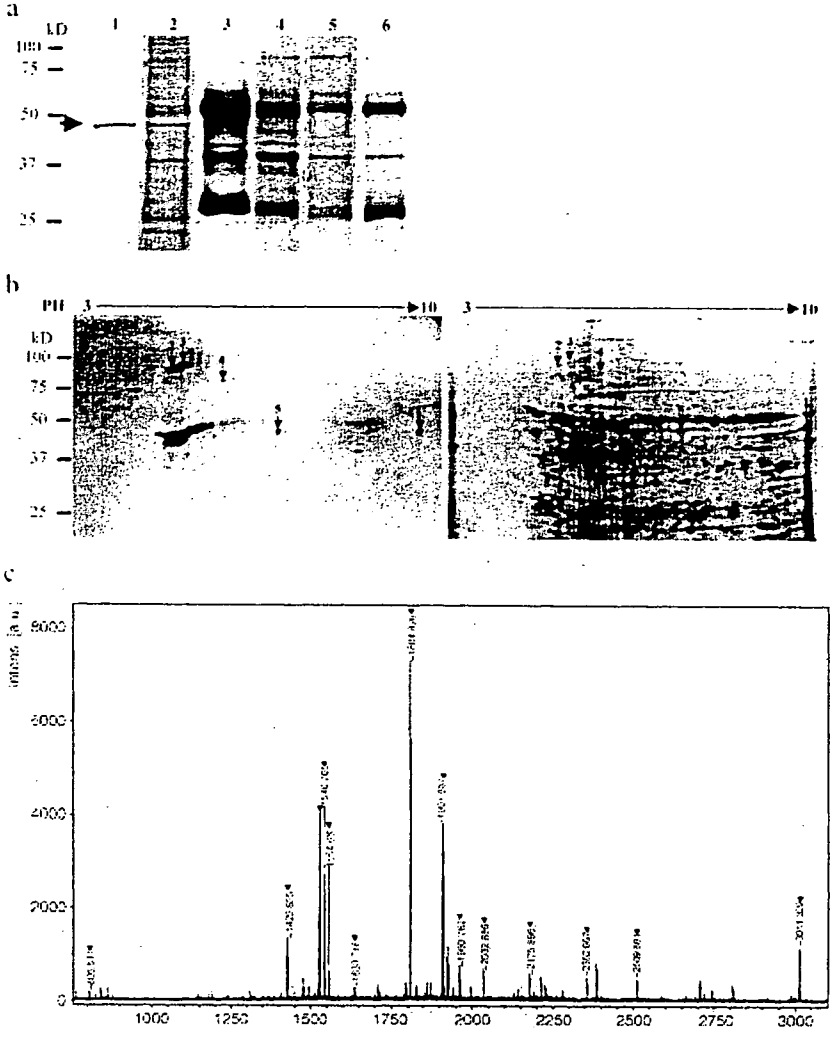

Fig. 1. (a) Screening by means of one-dimensional electrophoresis (1-DE) western blotting analysis for autoantigen associated with non-small cell lung cancer (NSCLC). Lane 1: ~47-kDa positive band (arrow), which was recognized by anti-enolase antibodies. Lanes 2, 3: 47-kDa positive band, which was recognized by NSCLC sera. Lane 4: no 47-kDa positive band was observed in a negative NSCLC case. Lane 5: no positive reaction was observed with healthy control sera. Lane 6: no positive reaction was observed in negative controls. (b) Detection by means of two-dimensional electrophoresis (2-DE) western blotting analysis of autoantigen associated with NSCLC. Left panel: Representative 2-DE western blotting analysis. Right panel: corresponding 2-DE silver-stained image. Protein spots recognized only by NSCLC sera are marked with arrows and numbers. (c) Peptide mass fingerprinting spectra of positive spot 5. For spot 5, 14 peptide masses were matched with human α-enolase by executing an NCBInr database search, yielding 52% protein sequence coverage. The matched mass peaks are marked with arrow heads.

Table 1. Mascot search results of the liquid chromatography-mass spectrometry/mass spectrometry (LC-MS/MS) data

Protein name	Swiss Prot Accession number	Molecular weight (Da)	pI	Score*	Peptide matched	Protein coverage (%)
Elongation factor 1-α 1	P68104	50 451	9.10	123	4	7
Cytokeratin 17	Q04695	48 230	4.97	271	13	25
α-Enolase	P06733	47 037	6.99	96	3	5
Elongation factor Tu	P49411	49 852	7.26	56	1	3
α-1-acid glycoprotein 1 precursor	P02763	23 725	4.93	160	4	18
Vimentin	P08670	53 545	5.06	115	5	9
Albumin precursor	P02768	71 317	5.92	106	4	6
Actin-like protein 3	P61158	47 797	5.61	46	2	7

*Scores > 39 indicate identity or extensive homology ($P < 0.05$). To identify the 47-kDa protein recognized only by non-small cell lung cancer patient sera, the corresponding band stained with Coomassie brilliant blue was digested and analyzed by LC-MS/MS. The eight proteins identified are listed.

are of similar molecular weight and one of them may be the autoantigen associated with NSCLC. We used western blotting with rabbit anti-enolase antibodies to confirm that the expression of α-enolase occurred at the same position as that of the 47-kDa positive band (Fig. 1a).

Autoantibodies against α-enolase present in NSCLC patient sera. To characterize autoantibodies in NSCLC sera, proteins extracted from a given patient's tumor tissue were separated by 2-DE, transferred to membranes, and incubated with sera from the same patient or from healthy control subjects. Compared with the sera of healthy control subjects, 2-DE western blotting with NSCLC patient sera showed five positive protein spots (Fig. 1b, left panel), including one spot (spot 5) that also had a molecular weight of approximately 47 kDa and a pI value of

doi: 10.1111/j.1349-7006.2007.00509.x

Table 2. Mascot search results of matrix-assisted laser desorption–ionization time-of-flight (MALDI-TOF) data

Spot no.	Protein name	Sequence coverage (%)	Molecular weight (Da)	pI
1	Chain D, myeloperoxidase	22	53 806	9.43
2	Tumor rejection antigen-1 (gp96)	17	92 696	4.76
3	Not identified			
4	α glucosidase II α subunit	15	86 236	5.71
5	α-enolase	52	47 037	6.99

To identify the immunoreactive spots in two-dimensional electrophoresis western blotting analysis recognized by non-small cell lung cancer patient sera, corresponding silver-stained spots were digested and analyzed by MALDI-TOF/mass spectrometry. 'Spot no.' corresponds to spots marked in Fig. 1b.

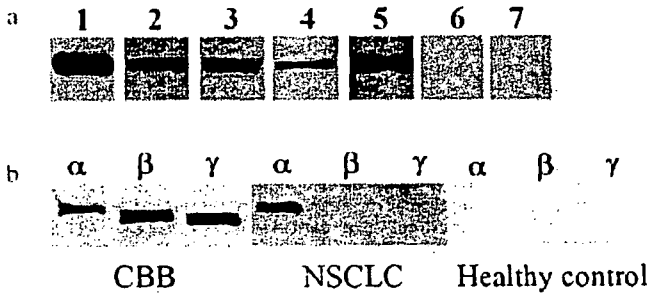

Fig. 2. (a) Western blotting analysis of recombinant human full-length α-enolase protein. Recombinant human full-length α-enolase protein was probed with rabbit anti-enolase antibodies (lane 1), with sera from non-small cell lung cancer (NSCLC) patients (lane 2–5), and with sera from healthy control subjects (lane 6–7). (b) Western blotting analysis of α, β and γ-enolase. α, β and γ-enolase protein were stained with Coomassie brilliant blue (left panel) or probed with sera from NSCLC patients (middle panel) and from healthy control subjects (right panel).

approximately 7.0. The corresponding spots on the silver-stained gel (Fig. 1b, right panel) were identified by MALDI-TOF/MS and database search. The identified proteins are summarized in Table 2. Spot 5 was recognized as α-enolase, as in the previous LC-MS/MS analysis. Its PMF spectrum is shown in Fig. 1c and the database search produced 14 peptide masses that coincided with human α-enolase, thus yielding 52% protein sequence coverage.

Next, western blotting with full-length recombinant human α-enolase protein was used to confirm and analyze the immunogenicity of α-enolase. Correct expression of the recombinant protein was verified by western blotting using rabbit anti-enolase antibodies (Fig. 2a). The recombinant proteins were then probed with sera from NSCLC patients or healthy control subjects, and positive bands were detected only in sera from the former, not from the latter (Fig. 2a). In addition, western blotting was used to determine the reactivity of NSCLC patient sera to enolase isoforms, which contain α, β and γ-enolase. The sera that were positive for autoantibodies against α-enolase reacted with neither β-enolase nor γ-enolase (Fig. 2b), whereas healthy control sera did not react with any of the enolase isoforms. This indicates the specificity of autoantibodies against α-enolase in NSCLC patient sera, and the overall results suggest that a subset of NSCLC patient sera contains autoantibodies against α-enolase.

Frequencies of autoantibodies against α-enolase in the sera were determined by means of ELISA using recombinant human full-length α-enolase protein. We tested 94 sera from patients with NSCLC, 15 from patients with SCLC, 18 from patients with gastrointestinal cancer (10 patients with gastric cancer, 8 patients with colon cancer), nine from patients with MAC infection of lung and 60 from healthy control subjects. When

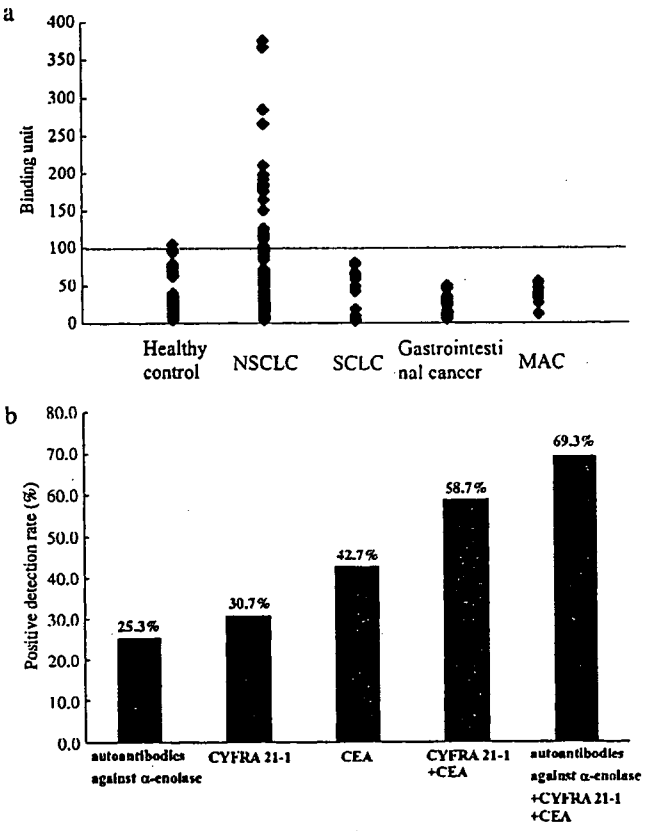

Fig. 3. (a) Prevalence of autoantibodies against α-enolase determined by enzyme-linked immunosorbent assay (ELISA). The *y*-axis denotes binding units. The solid horizontal line represents the positive cut-off limit. The prevalence of autoantibodies against α-enolase was 27.7% in patients with non-small cell lung cancer (NSCLC) (26 of 94), 1.7% in healthy control subjects (1 of 60), and not detectable in small cell lung cancer gastrointestinal cancer (10 patients with gastric cancer, 8 patients with colon cancer) and *Mycobacterium avium* complex infection of lung. (b) Positive detection rate of autoantibodies against α-enolase, cytokeratin 19 fragment (CYFRA21-1) and carcinoembryonic antigen (CEA) in NSCLC patients. Detection of CYFRA 21-1 and CEA in combination increased the positive detection rate to 58.7%. Furthermore, combined detection of autoantibodies against α-enolase, CEA and CYFRA 21-1 achieved a positive detection rate of up to 69.3%.

'Mean $OD_{\text{healthy control sera}} + 3\ SD_{\text{healthy control sera}}$' was used as the cut-off point, the prevalence of autoantibodies against α-enolase was 27.7% in patients with NSCLC (26 of 94), 1.7% in healthy control subjects (1 of 60), and not detectable in SCLC, gastrointestinal cancer or MAC infection of lung (Fig. 3a). These results

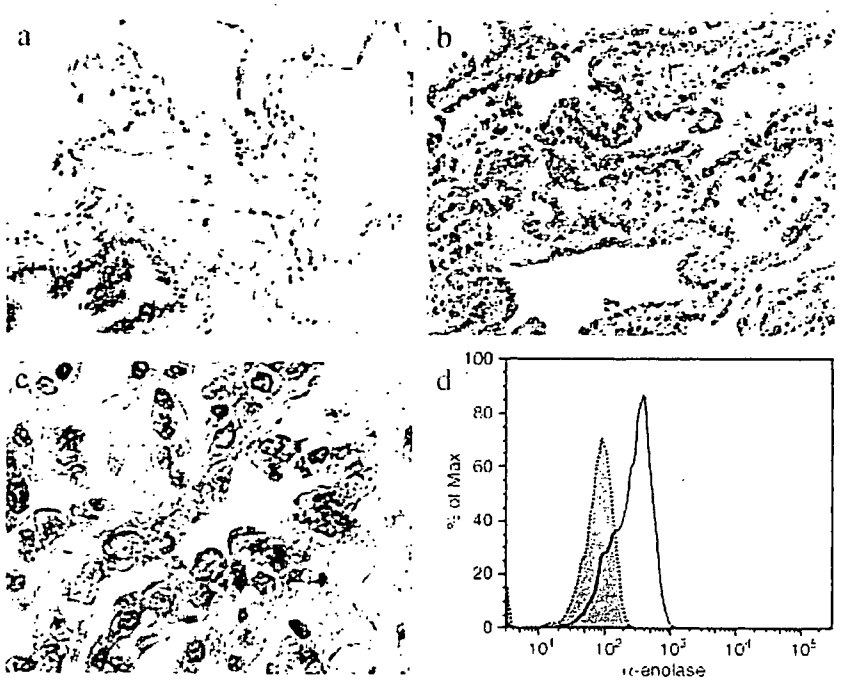

Fig. 4. Immunohistochemical and flow cytometric analysis of α-enolase. (a) Normal lung tissue (×100). (b) Lung adenocarcinoma (×100). (c) α-Enolase staining showing a mixture of cytoplasmic, and membranous immunoreactivity (×400). (d) A549 cells were stained with anti-enolase antibody, labeled with fluorescein-isothiocyanate-conjugated goat antirabbit immunoglobulin, and analyzed on a FACS Canto (open histogram). Shaded histogram indicates staining with control IgG.

showed that titers of autoantibodies against α-enolase are increased in a subset of NSCLC patients. Next, we examined the correlation between the prevalence of autoantibodies against α-enolase and clinicopathological features in NSCLC patients. Positive reactivity was detected in 21 of the 73 sera from adenocarcinoma patients (28.8%) and in five of the 21 sera from SCC patients (23.8%). There was no significant correlation between the occurrence of autoantibodies against α-enolase and pathological types ($P = 0.654$). In addition, there was a tendency for autoantibodies against α-enolase to be more prevalent in patients with advanced NSCLC cases (stage III/IV, 33.3%, 21 of 63) than in stage I/II cases (16.1%, 5 of 31), although the results of the statistical analysis suggest that the prevalence has no significant correlation with disease stage ($P = 0.08$). We also investigated the relationship between autoantibodies against α-enolase and other tumor markers (CEA, CYFRA 21-1) that have been applied to clinical practice in NSCLC patients. In a total of 94 NSCLC patients, clinical data of both CEA and CYFRA 21-1 were available for 75 patients. In these patients, 25.3% (19/75) were positive for autoantibodies against α-enolase, 42.7% (32/75) were positive for CEA, and 30.7% (23/75) were positive for CYFRA 21-1. The occurrence of autoantibodies against α-enolase didn't show a significant correlation with CEA ($P = 0.63$) or with CYFRA 21-1($P = 0.92$). Detection of CYFRA 21-1 and CEA in combination increased the positive detection rate to 58.7% (44/75). Furthermore, positive detection rate was enhanced up to 69.3% (52/75) when combined detection of autoantibodies against α-enolase, CEA and CYFRA 21-1 was used (Fig. 3b).

IHC and flow cytometric analysis of α-enolase. We used IHC staining to compare α-enolase expression in non-malignant and malignant lung tissues from 20 NSCLC patients, including 10 patients with autoantibodies against α-enolase and 10 patients without autoantibodies against α-enolase. The staining results showed that expression of α-enolase was increased in malignant lung tissue of NSCLC patients (Fig. 4a–c). Additionally, IHC staining showed not only cytoplasmic but also membranous immunoreactivity in cancer cells (Fig. 4c). Flow cytometric analysis of human lung adenocarcinoma cell line A549 also confirmed the expression of α-enolase at the surface of lung cancer cells (Fig. 4d).

Epitopes located at the N-terminal region (1–134 a.a.) of α-enolase that are recognized by autoantibodies. To locate the serological epitopes of α-enolase, full-length and C-terminal deletion mutant proteins (α-Eno1, α-Eno2, α-Eno3) were prepared. The full-length α-enolase (1–434 a.a.), α-Eno1 (1–334 a.a.), α-Eno2 (1–234 a.a.) and α-Eno3 (1–134 a.a.) recombinant proteins were clearly shown by an anti-6 × His antibody or stained with CBB, which verified their expression (Fig. 5). A commercially available rabbit anti-enolase antibody reacted only with the full-length α-enolase, α-Eno1 and α-Eno2 recombinant proteins (Fig. 5). However, sera from NSCLC patients who showed the presence of autoantibodies against α-enolase reacted with the α-Eno1, α-Eno2, and α-Eno3 recombinant proteins (Fig. 5), indicating that in NSCLC patients at least the N-terminal region of α-enolase contains epitopes.

Discussion

In the present study we used a proteomics-based screen test to identify proteins such as α-enolase and gp96 that may elicit a humoral immune response in NSCLC patients. We then confirmed that some NSCLC patients' sera contained autoantibodies against α-enolase by means of western blotting using recombinant protein. Furthermore, the results obtained with ELISA demonstrated that when 'Mean $OD_{\text{healthy control sera}} + 3\ SD_{\text{healthy control sera}}$' was used as the cut-off point, the humoral immune response directed against α-enolase occurred in 27.7% of NSCLC patients, but in only 1.7% of healthy control subjects. α-enolase is an isoenzyme of enolase, a key protein that catalyzes the conversion of 2-phosphoglycerate to phosphoenolpyruvate, which is the second of the two high-energy intermediates that generate ATP in glycolysis.[20] Three isoforms of enolase have been identified and are known as α, β and γ-enolase. α-enolase is present in most tissues and is predominant in early embryonic tissue, β-enolase is expressed in muscle tissue, and γ-enolase, also known as NSE, is found only in neuronal tissues.

Autoantibody responses to tumors are generally thought to be elicited in three ways. These are overexpression of specific proteins, especially on the cell surface, gene mutation or post-translational modification of proteins, which shows new epitopes

doi: 10.1111/j.1349-7006.2007.00509.x

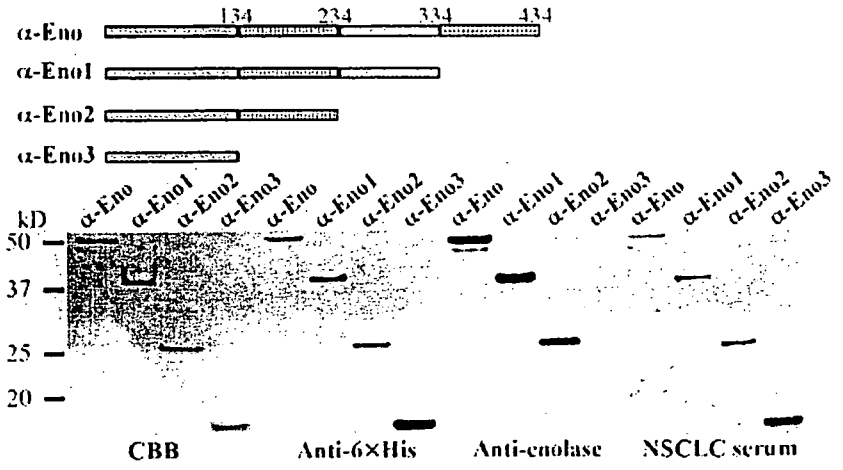

Fig. 5. Upper panel: preparation of recombinant human full-length α-enolase protein: α-Eno (1–434 a.a.), C-terminal deletion mutant α-enolase proteins: α-Eno1 (1–334 a.a.), α-Eno2 (1–234 a.a.) and α-Eno3 (1–134 a.a.). Lower panel: recombinant proteins were stained with Coomassie brilliant blue or probed with anti-6 x His antibody, anti-enolase antibody or non-small cell lung cancer sera.

as immunogens, and other types of protein processing in tumor tissue.[21] In the present study we used normal recombinant proteins to confirm the immunogenicity of α-enolase in NSCLC patients. In addition, although a past study reported that expression of α-enolase was downregulated in NSCLC tissues,[22] IHC staining used in our study showed that α-enolase expression is commonly increased in malignant lung tissue from NSCLC patients compared to the expression in non-malignant lung tissue, which is consistent with other previous reports.[23–27] Interestingly, IHC staining also showed not only cytoplasmic but also membranous immunoreactivity. Moreover, flow cytometric analysis demonstrated expression of α-enolase on the surface of lung cancer cells. We think that enhanced expression of α-enolase on cancer-cell surface might be one reason for autoantigenicity, and might be required for induction of autoantibody responses. However, α-enolase expression alone is insufficient for autoantibody production as increased expression was also found in these patients without autoantibodies against α-enolase. Further study is necessary to investigate the detailed mechanisms involved in this autoantibody response.

It is widely accepted that the propensity for glycolysis is enhanced in cancer cells because of increased cell proliferation. In fact, α-enolase, a key enzyme in the glycolysis pathway, was found to be overexpressed in 18 cancers.[25] Furthermore, although the mechanism of its surface expression and orientation on the membrane are not yet clearly understood, it is known that the C-terminal a.a. of α-enolase, lysine, is exposed at the cell surface and is involved in binding to plasminogen, which is then activated and converted to plasmin.[28] Once plasmin is stabilized at the cell surface, it in turn induces fibrinolysis.[20] In response to the upregulation of α-enolase expression, progression of the fibrinolytic system is markedly accelerated, and the resultant increase in local fibrinolysis may contribute to cancer cell invasion and metastasis. This is consistent with our finding that there was a tendency for autoantibodies against α-enolase to be more prevalent in patients with advanced NSCLC (stage III/IV) than in stage I/II cases.

Tumor markers for NSCLC are potentially useful for both diagnostic and therapeutic practice. To date, a variety of NSCLC tumor markers have been identified and the most extensively investigated circulating protein markers include CEA, CYFRA 21-1, SCC antigen, NSE and CA125.[5] The percentages of NSCLC patients who have elevated serum protein levels of the above markers are 26%–42% for CEA, 51%–74% for CYFRA 21-1, 20%–32% for SCC, 28–32% for NSE, and 46–55% for CA125, with variations depending on histology and stage.[5–8] However, because elevated serum protein levels of these markers have been observed in tumors other than NSCLC, their sensitivity and specificity are not satisfactory and their clinical applicability is limited. Our study demonstrated that when 'Mean $OD_{\text{healthy control sera}}$ + 3 $SD_{\text{healthy control sera}}$' was used as the cut-off point, autoantibodies against α-enolase occurred in 27.7% of NSCLC patients but not in those with SCLC, gastrointestinal cancer or MAC infection of the lungs. Moreover, combined detection of autoantibodies against α-enolase, CEA and CYFRA 21-1 enhanced sensitivity for the diagnosis of NSCLC. These results suggest that using autoantibodies against α-enolase has potential as a clinical biomarker for serological screening of NSCLC. Further large-scale validation studies will be needed to determine the sensitivity, specificity and positive prognostic value of this marker in real-world screening scenarios.

Autoantibodies against α-enolase have been detected in some autoimmune diseases,[20] and Fujii *et al.* report that in Hashimoto's encephalopathy one of these autoantibodies recognizes the N-terminal region of α-enolase.[29] Because our results show this same recognition in NSCLC, further experiments are warranted to compare epitopes in α-enolase as detected in NSCLC and in autoimmune diseases to determine its utility as a biomarker for NSCLC.

Acknowledgments

We would like to thank Dr S. Nomura for extremely helpful technical instructions for immunohistochemical staining. We also thank all members of our laboratory, especially Dr T. Hirano and Dr A. Ogata for their helpful discussions and support, and Ms T. Arimoto for her secretarial assistance. This study was supported by a Grant-in-Aid from the Ministry of Education, Science and Culture, Japan and the Osaka Foundation for Promotion of Clinical Immunology, Japan.

References

1 Jemal A, Siegel R, Ward E *et al.* Cancer statistics. *CA Cancer J Clin* 2006; 56: 106–30.
2 Stieber P, Aronsson AC, Bialk P *et al.* Tumor markers in lung cancer: EGTM recommendations. *Anticancer Res* 1999; 19: 2817–19.
3 Sidransky D. Emerging molecular markers of cancer. *Nat Rev Cancer* 2002; 2: 210–19.
4 Rastel D, Ramaioli A, Cornillie F, Thirion B. CYFRA 21-1, a sensitive and specific new tumor marker for squamous cell lung cancer. *Eur J Cancer* 1994; 30A: 601–6.
5 Trape J, Buxo J, Perez de Olaguer J, Vidal C. Tumor markers as prognostic

factors in treated non-small cell lung cancer. *Anticancer Res* 2003; 23: 4277–81.
6 Molina R, Agusti C, Mane JM *et al.* CYFRA 21-1 in lung cancer: comparison with CEA, CA 125, SCC and NSE serum levels. *Int J Biol Markers* 1994; 9: 96–101.
7 Lai RS, Hsu HK, Lu JY, Ger LP, Lai NS. CYFRA 21-1 enzyme-linked immunosorbent assay: Evaluation as a tumor marker in non-small cell lung cancer. *Chest* 1996; 109: 995–1000.
8 Kulpa J, Wojcik E, Reinfuss M, Kolodziejski L. Carcinoembryonic antigen, squamous cell carcinoma antigen, CYFRA 21-1, and neuron-specific enolase in squamous cell lung cancer patients. *Clin Chem* 2002; 48: 1931–7.
9 Yamamoto A, Shimizu E, Ogura T, Sone S. Detection of auto-antibodies against 1-myc oncogene products in sera from lung cancer patients. *Int J Cancer* 1996; 69: 283–9.
10 Yamamoto A, Shimizu E, Takeuchi E *et al.* Infrequent presence of anti-c-Myc antibodies and absence of c-Myc oncoprotein in sera from lung cancer patients. *Oncology* 1999; 56: 129–33.
11 Bergqvist M, Brattstrom D, Lamberg K *et al.* The presence of anti-p53 antibodies in sera prior to thoracic surgery in non small cell lung cancer patients: its implications on tumor volume, nodal involvement, and survival. *Neoplasia* 2003; 5: 283–7.
12 Blaes F, Klotz M, Huwer H *et al.* Antineural and antinuclear autoantibodies are of prognostic relevance in non-small cell lung cancer. *Ann Thorac Surg* 2000; 69: 254–8.
13 Brichory F, Beer D, Le Naour F, Giordano T, Hanash S. Proteomics-based identification of protein gene product 9.5 as a tumor antigen that induces a humoral immune response in lung cancer. *Cancer Res* 2001; 61: 7908–12.
14 Brichory FM, Misek DE, Yim AM *et al.* An immune response manifested by the common occurrence of annexins I and II autoantibodies and high circulating levels of IL-6 in lung cancer. *Proc Natl Acad Sci USA* 2001; 98: 9824–9.
15 Chang JW, Lee SH, Jeong JY *et al.* Peroxiredoxin-I is an autoimmunogenic tumor antigen in non-small cell lung cancer. *FEBS Lett* 2005; 579: 2873–7.
16 Humphrey LL, Teutsch S, Johnson M. US Preventive Services Task Force: lung cancer screening with sputum cytologic examination, chest radiography, and computed tomography: an update for the US Preventive Services Task Force. *Ann Intern Med* 2004; 140: 740–53.
17 Hanash S. Harnessing immunity for cancer marker discovery. *Nat Biotechnol* 2003; 21: 37–8.
18 Shevchenko A, Wilm M, Vorm O, Mann M. Mass spectrometric sequencing of proteins from silver-stained polyacrylamide gels. *Anal Chem* 1996; 68: 850–8.
19 Tsuruha J, Masuko-Hongo K, Kato T, Sakata M, Nakamura H, Nishioka K. Implication of cartilage intermediate layer protein in cartilage destruction in subsets of patients with osteoarthritis and rheumatoid arthritis. *Arthritis Rheum* 2001; 44: 838–45.
20 Pancholi V. Multifunctional α-enolase: its role in diseases. *Cell Mol Life Sci* 2001; 58: 902–20.
21 Imafuku Y, Omenn GS, Hanash S. Proteomics approaches to identify tumor antigen directed autoantibodies as cancer biomarkers. *Dis Markers* 2004; 20: 149–53.
22 Chang YS, Wu W, Walsh G, Hong WK, Mao L. Enolase-α is frequently down-regulated in non-small cell lung cancer and predicts aggressive biological behavior. *Clin Cancer Res* 2003; 9: 3641–4.
23 Chen G, Gharib TG, Wang H *et al.* Protein profiles associated with survival in lung adenocarcinoma. *Proc Natl Acad Sci USA* 2003; 100: 13 537–42.
24 Li LS, Kim H, Rhee H *et al.* Proteomic analysis distinguishes basaloid carcinoma as a distinct subtype of non-small cell lung carcinoma. *Proteomics* 2004; 4: 3394–400.
25 Altenberg B, Greulich KO. Genes of glycolysis are ubiquitously overexpressed in 24 cancer classes. *Genomics* 2004; 84: 1014–20.
26 Li C, Xiao Z, Chen Z *et al.* Proteome analysis of human lung squamous carcinoma. *Proteomics* 2006; 6: 547–58.
27 Chang GC, Liu KJ, Hsieh CL *et al.* Identification of α-enolase as an autoantigen in lung cancer: its overexpression is associated with clinical outcomes. *Clin Cancer Res* 2006; 12: 5746–54.
28 Redlitz A, Fowler BJ, Plow EF, Miles LA. The role of an enolase-related molecule in plasminogen binding to cells. *Eur J Biochem* 1995; 227: 407–15.
29 Fujii A, Yoneda M, Ito T *et al.* Autoantibodies against the amino terminal of α-enolase are a useful diagnostic marker of Hashimoto's encephalopathy. *J Neuroimmunol* 2005; 162: 130–6.

doi: 10.1111/j.1349-7006.2007.00509.x

Differential Constitutive Activation of the Epidermal Growth Factor Receptor in Non–Small Cell Lung Cancer Cells Bearing *EGFR* Gene Mutation and Amplification

Takafumi Okabe,[1] Isamu Okamoto,[1] Kenji Tamura,[3] Masaaki Terashima,[1] Takeshi Yoshida,[1] Taroh Satoh,[1] Minoru Takada,[2] Masahiro Fukuoka,[1] and Kazuhiko Nakagawa[1]

[1]Department of Medical Oncology, Kinki University School of Medicine; [2]National Kinki Central Chest Medical Center, Osaka, Japan; and [3]Department of Medical Oncology, Nara Hospital, Kinki University School of Medicine, Nara, Japan

Abstract

The identification of somatic mutations in the tyrosine kinase domain of the epidermal growth factor receptor (EGFR) in patients with non–small cell lung cancer (NSCLC) and the association of such mutations with the clinical response to EGFR tyrosine kinase inhibitors (TKI), such as gefitinib and erlotinib, have had a substantial effect on the treatment of this disease. *EGFR* gene amplification has also been associated with an increased therapeutic response to EGFR-TKIs. The effects of these two types of *EGFR* alteration on EGFR function have remained unclear, however. We have now examined 16 NSCLC cell lines, including eight newly established lines from Japanese NSCLC patients, for the presence of *EGFR* mutations and amplification. Four of the six cell lines that harbor *EGFR* mutations were found to be positive for *EGFR* amplification, whereas none of the 10 cell lines negative for *EGFR* mutation manifested *EGFR* amplification, suggesting that these two types of *EGFR* alteration are closely associated. Endogenous EGFRs expressed in NSCLC cell lines positive for both *EGFR* mutation and amplification were found to be constitutively activated as a result of ligand-independent dimerization. Furthermore, the patterns of both *EGFR* amplification and EGFR autophosphorylation were shown to differ between cell lines harboring the two most common types of *EGFR* mutation (exon 19 deletion and L858R point mutation in exon 21). These results reveal distinct biochemical properties of endogenous mutant forms of EGFR expressed in NSCLC cell lines and may have implications for treatment of this condition. [Cancer Res 2007;67(5):2046–53]

Introduction

The epidermal growth factor receptor (EGFR) is a 170-kDa transmembrane glycoprotein with an extracellular ligand binding domain, a transmembrane region, and a cytoplasmic tyrosine kinase domain and is encoded by a gene (*EGFR*) located at human chromosomal region 7p12 (1–3). The binding of ligand to EGFR induces receptor dimerization and consequent conformational changes that result in activation of the intrinsic tyrosine kinase, receptor autophosphorylation, and activation of a signaling cascade (4, 5). Aberrant signaling by EGFR plays an important role in cancer development and progression (3).

EGFR is frequently overexpressed in non–small cell lung cancer (NSCLC) and has been implicated in the pathogenesis of this disease (6, 7). Given the biological importance of EGFR signaling in cancer, several agents have been synthesized that inhibit the receptor tyrosine kinase activity. Two such inhibitors of the tyrosine kinase activity of EGFR (EGFR-TKI), gefitinib and erlotinib, both of which compete with ATP for binding to the tyrosine kinase pocket of the receptor, have been extensively studied in patients with NSCLC (8, 9). We and others have shown that a clinical response to these agents is more common in women than in men, in Japanese than in individuals from Europe or the United States, in patients with adenocarcinoma than in those with other histologic subtypes of cancer, and in patients who have never smoked than in those with a history of smoking (10–14). Mutations in the tyrosine kinase domain of EGFR have also been detected in a subset of lung cancer patients and shown to predict sensitivity to EGFR-TKIs (15–17). Indeed, the clinical characteristics of patients with known *EGFR* mutations are similar to those of other individuals most likely to respond to treatment with EGFR-TKIs (18–22). These mutations arise in the first four exons (exons 18–21) corresponding to the tyrosine kinase domain of EGFR, and they affect key amino acids surrounding the ATP-binding cleft (23, 24). In-frame deletions that eliminate four highly conserved amino acids (LREA) encoded by exon 19 are the most common type of *EGFR* mutation, with missense point mutations in exon 21 that result in a specific amino acid substitution at position 858 (L858R) being the second most common. In addition to *EGFR* mutations, other molecular changes may play a role in determining sensitivity to EGFR-TKIs (22, 25–28). NSCLC patients with an increased *EGFR* copy number, as revealed by fluorescence *in situ* hybridization (FISH), have thus been found to show an increased response rate to and prolonged survival after gefitinib therapy (22, 25–27).

Given that *EGFR* is mutated or amplified (or both) in NSCLC, it is important to determine the biological effects of such *EGFR* alterations on EGFR function (15, 29–32). Transient transfection of various cell types with vectors encoding wild-type or mutant versions of EGFR showed that the activation of mutant receptors by EGF is more pronounced and sustained than is that of the wild-type receptor (15, 30). However, detailed biochemical analysis of NSCLC cell lines with endogenous *EGFR* mutations has been limited. We have now identified *EGFR* mutations in three NSCLC cell lines newly established from Japanese patients. Furthermore, we have characterized a panel of 16 NSCLC cell lines for *EGFR* mutations and amplification and evaluated the relation between the presence of these two types of *EGFR* alteration and sensitivity to gefitinib. The effects of *EGFR* alterations on activation status of EGFR and on downstream signaling were also evaluated.

Requests for reprints: Isamu Okamoto, Department of Medical Oncology, Kinki University School of Medicine, 377-2, Ohno-higashi, Osaka-Sayama, Osaka 589-8511, Japan. Phone: 81-72-366-0221; Fax: 81-72-360-5000; E-mail: okamoto@dotd.med.kindai.ac.jp.

doi:10.1158/0008-5472.CAN-06-3339

Finally, in *EGFR* mutant cell lines showing constitutive EGFR activation, we assessed how the mutations activate the tyrosine kinase domain of the receptor.

Materials and Methods

Cell lines. The human NSCLC cell lines NCI-H226 (H226), NCI-H292 (H292), NCI-H460 (H460), NCI-H1299 (H1299), NCI-H1650 (H1650), and NCI-H1975 (H1975) were obtained from the American Type Culture Collection (Manassas, VA). PC-9 and A549 cells were obtained as described previously (33). Ma-1 cells were kindly provided by E. Shimizu (Tottori University, Yonago, Japan). We established seven cell lines (KT-2, KT-4, Ma-25, Ma-31, Ma-34, Ma-45, and Ma-53) from tissue or pleural effusion of Japanese patients with advanced NSCLC. These cell lines were cultured under a humidified atmosphere of 5% CO_2 at 37°C in RPMI 1640 (Sigma, St. Louis, MO) supplemented with 10% fetal bovine serum. Informed consent for establishment of cell lines and tumor DNA sequencing was obtained in accordance with the ethical guidelines for human genome/genetic analysis in Japan.

Growth inhibition assay. Gefitinib was kindly provided by AstraZeneca (Macclesfield, United Kingdom) as a pure substance and was diluted in DMSO to obtain a stock solution of 20 mmol/L. For growth inhibition assays, cells (0.5×10^4 to 4.5×10^4) were plated in 96-well flat-bottomed plates and cultured for 24 h before the addition of various concentrations of gefitinib and incubation for an additional 72 h. TetraColor One (5 mmol/L tetrazolium monosodium salt and 0.2 mmol/L 1-methoxy-5-methyl phenazinium methylsulfate; Seikagaku, Tokyo, Japan) was then added to each well, and the cells were incubated for 3 h at 37°C before measurement of absorbance at 490 nm with a Multiskan Spectrum instrument (Thermo Labsystems, Boston, MA). Absorbance values were expressed as a percentage of that for untreated cells, and the concentration of gefitinib resulting in 50% growth inhibition (IC_{50}) was calculated.

Genetic analysis of *EGFR*. Genomic DNA was extracted from cell lines with the use of a QIAamp DNA Mini kit (Qiagen, Tokyo, Japan), and exons 18 to 21 of *EGFR* were amplified by the PCR and sequenced directly. PCR was done in a reaction mixture (25 μL) containing 50 ng of genomic DNA and TaKaRa Taq polymerase (TaKaRa BIO, Tokyo, Japan) and with an initial incubation for 3 min at 94°C followed by 30 cycles of 20 s at 94°C, 30 s at 58°C, and 20 s at 72°C and by a final incubation for 7 min at 72°C. The PCR products were purified with a Microcon YM-100 filtration device (Millipore, Billerica, MA) before sequencing with the use of an ABI BigDye Terminator v. 3.1 Cycle Sequencing kit (Applied Biosystems, Foster City, CA). Sequencing reaction mixtures were subjected to electrophoresis with an ABI PRISM 3100 Genetic Analyzer (Applied Biosystems). Primers for mutation analysis (sense and antisense, respectively) were as follows: exon 18, 5′-CAAATGAGCTGGCAAGTGCCGTGTC-3′ and 5′-GAGTTTCCCAAACACTCAGTGAAA-C-3′; exon 19, 5′-GCAATATCAGCCTTAGGTGCGGCTC-3′and 5′-CATAGAAAGTGAACATTTAGGATGTG-3′; exon 20, 5′-CCATGAGTACGTATTTTGAAACTC-3′ and 5′-CATATCCCCATGGCAAACTCTTGC-3′; and exon 21, 5′-CTAACGTTCGCCAGCCATAAGTCC-3′ and 5′-GCTGCGAGCTCACCCAGAATGTCTGG-3′.

FISH. *EGFR* copy number per cell was determined by FISH with the use of the LSI EGFR Spectrum Orange and CEP7 Spectrum Green probes (Vysis; Abbott, Des Plaines, IL). Cells were centrifuged onto glass slides with a Shandon cytocentrifuge (Thermo Electron, Pittsburgh, PA) and fixed by consecutive incubations with ice-cold 70% ethanol for 10 min, 85% ethanol for 5 min, and 100% ethanol for 5 min. Slides were stored at −20°C until analysis. Cells were subsequently subjected to digestion with pepsin for 10 min at 37°C, washed with water, dehydrated with a graded series of ethanol solutions, denatured with 70% formamide in 2× SSC for 5 min at 72°C, and dehydrated again with a graded series of ethanol solutions before incubation with a hybridization mixture consisting of 50% formamide, 2× SSC, Cot-1 DNA, and labeled DNA. The slides were washed for 5 min at 73°C with 3× SSC, for 5 min at 37°C with 4× SSC containing 0.1% Triton X-100, and for 5 min at room temperature with 2× SSC before counterstaining with antifade solution containing 4′,6-diamidino-2-phenylindole. Hybridization signals were scored in 40 nuclei with the use of a ×100 immersion objective. Nuclei with a disrupted boundary were excluded from the analysis. Gene amplification was defined by an *EGFR*/chromosome 7 copy number ratio of ≥2 or by the presence of clusters of ≥15 copies of *EGFR* per cell in ≥10% of cells, as described previously (25, 27).

Immunoblot analysis. Cell lysates were fractionated by SDS-PAGE on a 7.5% gel, and the separated proteins were transferred to a nitrocellulose membrane. After blocking of nonspecific sites with 5% skim milk, the membrane was incubated overnight at room temperature with primary antibodies. Antibodies to phosphorylated EGFR (pY845, pY1068, or pY1173), extracellular signal-regulated kinase (ERK), phosphorylated AKT, AKT, Src homology and collagen (Shc), and phosphorylated Shc were obtained from Cell Signaling Technology (Beverly, MA); antibodies to EGFR were from Zymed (South San Francisco, CA); antibodies to phosphorylated ERK were from Santa Cruz Biotechnology (Santa Cruz, CA); and antibodies to β-actin (loading control) were from Sigma. Immune complexes were detected by incubation of the membrane for 1 h at room temperature with horseradish peroxidase–conjugated goat antibodies to mouse or rabbit immunoglobulin (Amersham Biosciences, Little Chalfont, United Kingdom) and by subsequent exposure to enhanced chemiluminescence reagents (Perkin-Elmer, Boston, MA).

Table 1. Characteristics of NSCLC cell lines

Cell lines	Gefitinib IC_{50} (μmol/L)	*EGFR* mutation	*EGFR* amplification	Histology
PC-9	0.07	del(E746-A750)	+	Adenocarcinoma
KT-2	0.57	L858R	+	Adenocarcinoma
KT-4	1.26	L858R	+	Large cell carcinoma
Ma-1	2.34	del(E746-A750)	+	Adenocarcinoma
H1650	6.66	del (E746-A750)	−	Adenocarcinoma
A549	8.70	Wild type	−	Adenocarcinoma
H1975	9.32	L858R+T790M	−	Adenocarcinoma
H292	9.44	Wild type	−	Mucoepidermoid carcinoma
H226	9.53	Wild type	−	Squamous cell carcinoma
Ma-25	10.17	Wild type	−	Large cell carcinoma
H460	10.38	Wild type	−	Large cell carcinoma
Ma-45	10.47	Wild type	−	Adenocarcinoma
Ma-53	10.47	Wild type	−	Adenocarcinoma
Ma-34	11.17	Wild type	−	Adenocarcinoma
H1299	11.28	Wild type	−	Large cell carcinoma
Ma-31	12.46	Wild type	−	Adenocarcinoma

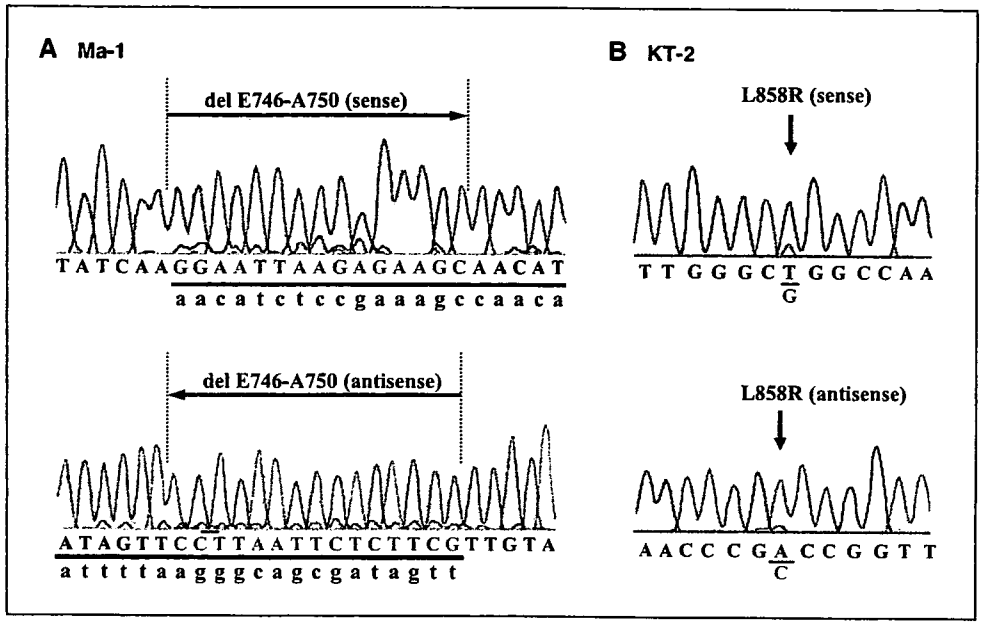

Figure 1. Detection of *EGFR* mutations in NSCLC cell lines. The portions of the sequencing electrophoretograms corresponding to the mutations are shown for Ma-1 (*A*) and KT-2 (*B*) cells. *A*, heterozygous in-frame deletion in exon 19 is revealed by the presence of double peaks. Tracings in both sense and antisense directions are shown to highlight the two breakpoints of the deletion. Wild-type (*uppercase*) and mutant (*lowercase*) nucleotide sequences. *B*, heterozygous point mutation (T → G) at nucleotide position 2819 in exon 21.

Treatment of cells with neutralizing antibodies. Cells were exposed to neutralizing antibodies (each at 12 μg/mL) for 3 h before EGF stimulation. The antibodies included those to EGF and to transforming growth factor-α (TGF-α), both from R&D Systems (Minneapolis, MN) as well as antibodies to EGFR (Upstate Biotechnology, Lake Placid, NY). Cell lysates were then prepared and subjected to immunoblot analysis with antibodies to phosphorylated EGFR (pY1068) and to EGFR as described above.

Chemical cross-linking assay. Chemical cross-linking was done as described previously (34, 35). Cells were washed twice with ice-cold PBS and then incubated for 20 min at 4°C with 1 mmol/L bis(sulfosuccinimidyl)-suberate (Pierce, Rockford, IL) in PBS. The cross-linking reaction was terminated by the addition of glycine to a final concentration of 250 mmol/L and incubation for an additional 5 min at 4°C. The cells were washed with PBS, and cell lysates were resolved by SDS-PAGE on a 4% gel and subjected to immunoblot analysis with anti-EGFR (Santa Cruz Biotechnology).

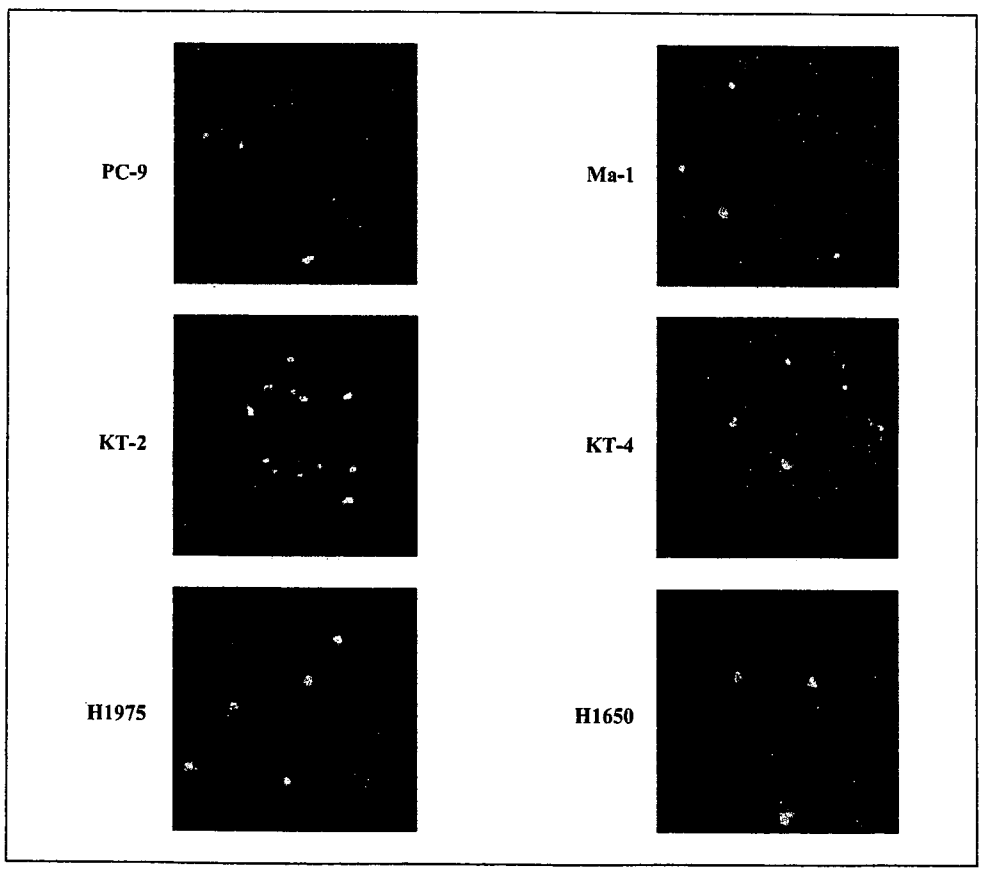

Figure 2. FISH analysis of *EGFR* amplification in NSCLC cell lines. The analysis was done with probes specific for *EGFR* (*red signals*) and for the centromere of chromosome 7 (*green signals*) in the indicated cell lines. PC-9 and Ma-1 cells manifest an *EGFR*/chromosome copy number ratio of ≥2, whereas KT-2 and KT-4 cells manifest *EGFR* clusters. H1975 and H1650 cells are negative for *EGFR* amplification.

Results

Effect of gefitinib on the growth of NSCLC cell lines. We first examined the effect of the EGFR-TKI gefitinib on the growth of 16 NSCLC cell lines, eight of which (KT-2, KT-4, Ma-1, Ma-25, Ma-31, Ma-34, Ma-45, and Ma-53) were established from Japanese NSCLC patients for the present study. The IC_{50} values for gefitinib chemosensitivity ranged from 0.07 to 12.46 μmol/L (a 178-fold difference; Table 1).

Four cell lines (PC-9, KT-2, KT-4, and Ma-1) were relatively sensitive to gefitinib with IC_{50} values between 0.07 and 2.34 μmol/L, whereas the remaining 12 lines were considered resistant to gefitinib (IC_{50} > 6 μmol/L). No relation was apparent between sensitivity to gefitinib and histologic subtype of NSCLC for this panel of cell lines (Table 1).

***EGFR* mutation and amplification in NSCLC cell lines.** We screened the 16 NSCLC cell lines for the presence of *EGFR* mutations in exons 18 to 21, which encode the catalytic domain of the receptor. As previously described (36–39), PC-9, H1650, and H1975 cell lines were found to harbor *EGFR* mutations [del(E746-A750) in PC-9 and H1650 and both L858R and T790M in H1975]. Furthermore, we detected *EGFR* mutations in three of the newly established cell lines (Ma-1, KT-2, and KT-4). Ma-1 cells, which were isolated from a female ex smoker with adenocarcinoma (>30 years of age), were found to harbor a small deletion within exon 19 [del(E746-A750); Fig. 1*A*; Table 1]. Both KT-2 cells [derived from a male ex smoker with adenocarcinoma (>30 years of age)] and KT-4 cells (derived from a male nonsmoker with large cell carcinoma) harbor a point mutation (L858R) in exon 21 (Fig. 1*B*; Table 1). Four of these six NSCLC cell lines with *EGFR* mutations (PC-9, Ma-1, KT-2, and KT-4) are sensitive to gefitinib (Table 1), consistent with clinical observations (15–17, 20, 22).

We next examined the 16 NSCLC cell lines for the presence of *EGFR* amplification by FISH analysis with a probe specific for *EGFR* and a control probe for the centromere of chromosome 7. Four (PC-9, Ma-1, KT-2, and KT-4) of the 16 cell lines, all of which harbor *EGFR* mutations, were found to be positive for *EGFR* amplification (Fig. 2; Table 1). PC-9 and Ma-1 cell lines, both of which harbor the same exon 19 deletion, showed an *EGFR*/chromosome copy number ratio of ≥2, whereas KT-2 and KT-4, both of which harbor the L858R mutation in exon 21, showed a clustered unbalanced gain of *EGFR* copy number (Fig. 2). The four cell lines that manifested both *EGFR* mutation and amplification were sensitive to gefitinib (Table 1). The *EGFR* mutant cell lines H1650 and H1975 showed no evidence of *EGFR* amplification (Fig. 2), and both of these lines were relatively resistant to gefitinib (Table 1). None of the cell lines negative for *EGFR* mutations manifested *EGFR* amplification (Table 1), suggesting that *EGFR* mutation is closely associated with *EGFR* amplification ($P < 0.05$, χ^2 test).

EGFR expression in NSCLC cell lines. We examined the basal abundance of EGFR in *EGFR* wild-type and mutant NSCLC cell lines by immunoblot analysis. The amount of EGFR in the cell lines PC-9, Ma-1, KT-2, and KT-4, all of which manifest *EGFR* amplification and *EGFR* mutation, was increased compared with that in *EGFR* wild-type cell lines (A549 and H1299) or *EGFR* mutant cell lines negative for *EGFR* amplification (H1975 and H1650; Fig. 3). These results, thus, reveal a close relation between increased EGFR expression and *EGFR* amplification in this panel of NSCLC cell lines, consistent with the results of previous analyses of NSCLC tissue specimens (6, 7).

EGFR phosphorylation in NSCLC cell lines. We examined tyrosine phosphorylation of endogenous EGFRs in NSCLC cell lines by immunoblot analysis with phosphorylation site–specific antibodies. In cells (A549) that express only wild-type EGFR, phosphorylation of the receptor at Y845, Y1068, or Y1173 was undetectable in the absence of EGF but was markedly induced on

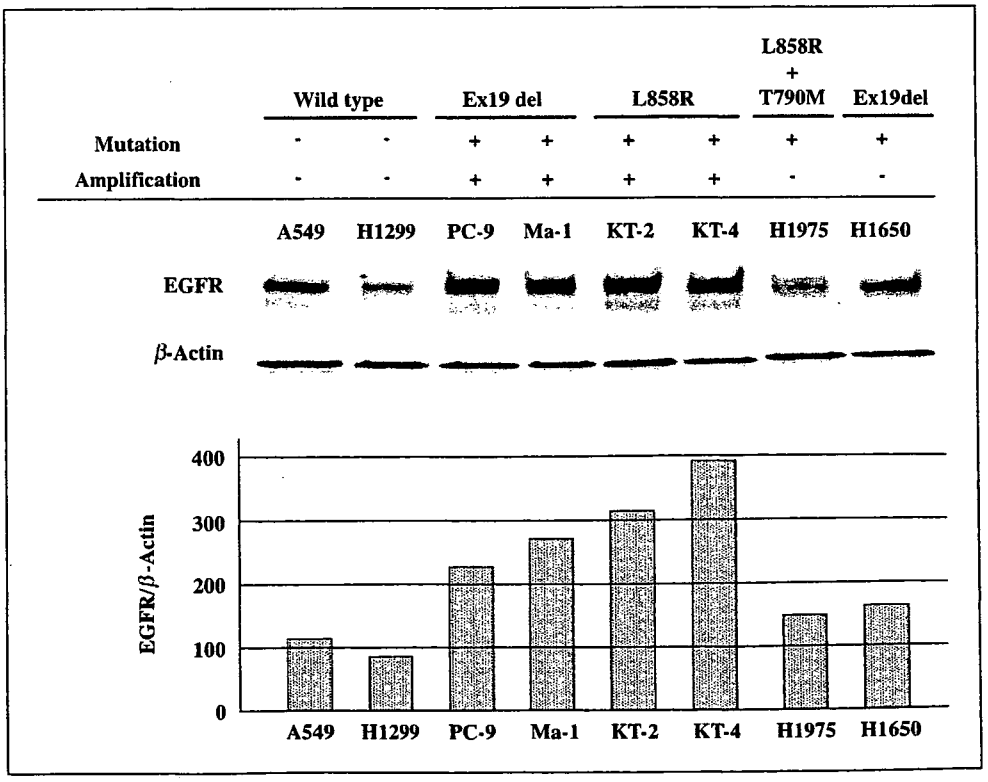

Figure 3. EGFR expression in NSCLC cell lines. Lysates (40 μg of protein) of NSCLC cell lines positive or negative for *EGFR* mutation or amplification, as indicated, were subjected to immunoblot analysis with antibodies to EGFR and to β-actin (*top*). The abundance of EGFR relative to that of β-actin was determined by densitometry (*bottom*). Representative of three independent experiments.

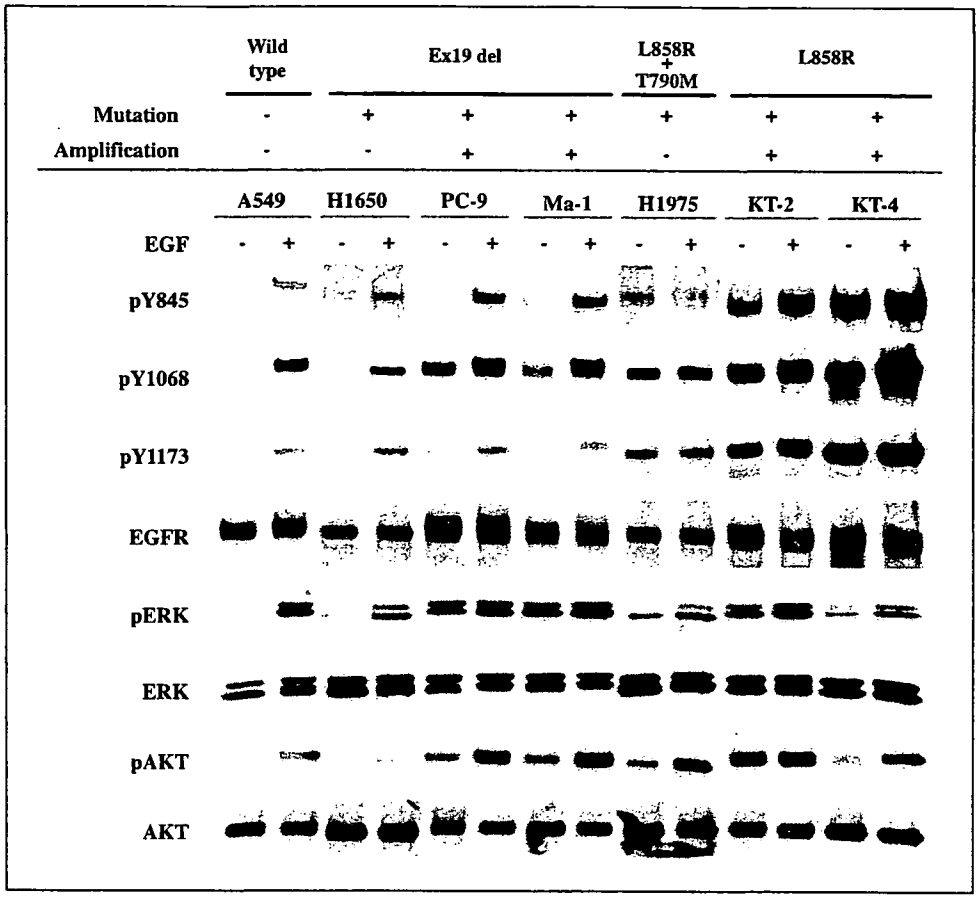

Figure 4. Phosphorylation of EGFR and downstream signaling molecules in NSCLC cell lines. Serum-deprived cells were incubated for 15 min in the absence or presence of EGF (100 ng/mL), after which cell lysates (40 μg of protein) were subjected to immunoblot analysis with antibodies to phosphorylated forms of EGFR (*pEGFR*), ERK (*pERK*), or AKT (*pAKT*) as well as antibodies to all forms of the corresponding proteins, as indicated. Representative of three independent experiments.

exposure of the cells to this growth factor (Fig. 4). Similar results were obtained with H1650 cells, which are positive for the deletion in exon 19 of *EGFR* but negative for *EGFR* amplification. In contrast, PC-9 and Ma-1 cells, which are positive for both the exon 19 deletion and *EGFR* amplification, manifested an increased basal level of EGFR phosphorylation at Y1068, indicative of constitutive activation of the EGFR tyrosine kinase. Exposure of PC-9 or Ma-1 cells to EGF induced EGFR phosphorylation at Y845 and Y1173, showing that the mutant receptors remain sensitive to ligand stimulation. Furthermore, the cell lines (H1975, KT-2, and KT-4) with the L858R point mutation manifested an increased basal level of EGFR phosphorylation at Y845, Y1068, and Y1173, and the extent of phosphorylation at these residues was increased only slightly by treatment of the cells with EGF, indicative of constitutive activation of the EGFR tyrosine kinase. These results thus showed that endogenous *EGFR* mutations result in constitutive receptor activation, and that the patterns of tyrosine phosphorylation of EGFR differ between the two most common types of *EGFR* mutant.

Phosphorylation of signaling molecules downstream of EGFR in NSCLC cell lines. Given that constitutive activation of EGFR was detected in NSCLC cell lines with endogenous *EGFR* mutations, we examined whether signaling molecules that act downstream of the receptor are also constitutively activated in these cell lines. We first examined the basal levels of phosphorylation of AKT and ERK, both of which mediate the oncogenic effects of EGFR. Immunoblot analysis with antibodies to phosphorylated forms of AKT or ERK revealed that these molecules are indeed constitutively activated in the *EGFR* mutant lines (PC-9, Ma-1, H1975, KT-2, and KT-4) that manifest constitutive activation of EGFR, although the extent of phosphorylation varied (Fig. 4). The increased levels of AKT and ERK phosphorylation in these mutant cell lines are consistent with the increased level of EGFR phosphorylation on Y1068, which serves as the docking site for phosphatidylinositol 3-kinase and growth factor receptor binding protein 2, molecules that mediate the activation of AKT and the Ras-ERK pathway, respectively (2, 40). We next examined whether the differences in the pattern of constitutive tyrosine phosphorylation of EGFR apparent between NSCLC cell lines harboring the exon 19 deletion and those with the L858R mutation in exon 21 are associated with distinct alterations in downstream signaling pathways. Given that Y1173, a major docking site of EGFR for the adapter protein Shc (2, 40, 41), is constitutively phosphorylated in cells with the L858R mutation but not in those with the exon 19 deletion, we compared Shc phosphorylation between cell lines with these two types of *EGFR* mutation. Ligand-independent tyrosine phosphorylation of the 52- and 46-kDa isoforms of Shc was apparent in cell lines with either type of *EGFR* mutation (Fig. 5). However, cell lines (KT-2 and KT-4) that harbor the L858R mutation exhibited a markedly greater basal level of phosphorylation of the 66-kDa isoform of Shc than did those (PC-9 and Ma-1) that harbor the exon 19 deletion or those (A549) that harbor only wild-type *EGFR*. These data suggest that the constitutively active mutant forms of *EGFR* induce selective activation of downstream effectors as a result of differential patterns of receptor autophosphorylation.

Ligand-independent dimerization and activation of *EGFR* mutants. Evidence suggests that EGFR ligands, including EGF and TGF-α, secreted by tumor cells themselves might be responsible for activation of mutant receptors in an autocrine loop (29, 42). To investigate whether EGFR is constitutively activated as a result of such an autocrine mechanism in *EGFR* mutant NSCLC cell lines, we treated the cells with a combination of three neutralizing antibodies (anti-EGF, anti-TGF-α, and anti-EGFR) for 3 h and then examined the effect of EGF on EGFR phosphorylation. The ligand-dependent activation of EGFR in A549 cells (which express only wild-type *EGFR*) was blocked by such antibody treatment (Fig. 6*A*). In contrast, treatment of the *EGFR* mutant cell lines PC-9 or KT-4 with the neutralizing antibodies failed to inhibit the constitutive phosphorylation of EGFR on Y1068. These observations suggest that the constitutive phosphorylation of the mutant receptors is not attributable to autocrine stimulation, although we are not able to exclude a possible role for other EGFR ligands.

Ligand-induced EGFR dimerization is responsible for activation of the receptor tyrosine kinase (4, 5). To determine whether mutant receptors are constitutively dimerized, we treated *EGFR* wild-type or mutant cell lines with a cross-linking agent before immunoblot analysis with antibodies to EGFR. Whereas ligand-induced dimerization of wild-type *EGFR* was observed in A549 cells, receptor dimerization in PC-9 and KT-4 cells, which express mutant receptors, was apparent in the absence of ligand and was not increased substantially by exposure of the cells to EGF (Fig. 6*B*). These data indicate that ligand-independent receptor dimerization is responsible for the constitutive activation of the mutant forms of *EGFR*.

Discussion

The discovery of somatic mutations in the tyrosine kinase domain of EGFR and of their association with a high response rate to EGFR-TKIs has had a substantial effect on the treatment of advanced NSCLC (15–17, 20, 22). Asian patients with NSCLC seem to have a higher prevalence of these mutations, ranging from 20% to 40% (18, 20, 21, 43–45). We have now identified *EGFR* mutations in three of eight newly established cell lines from Japanese patients with advanced NSCLC. Characterization of these eight new cell lines and eight previously established NSCLC lines revealed that, consistent with previous observations (29, 31, 36), those cell lines that harbor *EGFR* mutations are more likely to be sensitive to gefitinib than are those without such mutations. Not all *EGFR* mutant cell lines (e.g., H1650 and H1975) are sensitive to this EGFR-TKI, however, suggesting the existence of additional determinants of gefitinib sensitivity. In addition to the L858R mutation in exon 21 of *EGFR*, H1975 cells contain the T790M mutation in exon 20, which has been shown to confer resistance to EGFR-TKIs (38, 39). H1650 cells, which do not harbor mutations in *EGFR* other than the exon 19 deletion, manifest loss of the tumor suppressor phosphatase and tensin homologue deleted on chromosome 10 (37), which may result in resistance to EGFR-TKIs. *EGFR* amplification in NSCLC cells has also been shown to correlate with a better response to gefitinib (22, 25–27). Given that little is known of the relation between *EGFR* mutation and amplification in NSCLC, we examined the 16 NSCLC cell lines used in this study for *EGFR* amplification by FISH. Four of the six cell lines with *EGFR* mutations were found to be positive for gene amplification, whereas none of the 10 mutation-negative cell lines manifested *EGFR* amplification. This finding thus suggests that *EGFR* mutation and amplification are linked. Cappuzzo et al. showed that 6 of 9 (67%) NSCLC patients with *EGFR* amplification also had *EGFR* mutations (25). Furthermore, Takano et al. sequenced *EGFR* and determined the *EGFR* copy number by real-time PCR analysis for the tumors of 66 NSCLC patients (22); all of the patients with a high *EGFR* copy number (≥6.0 per cell) also had *EGFR* mutations. Moreover, PCR analysis revealed selective amplification of the mutant *EGFR* alleles in the patients with a high *EGFR* copy number. Our sequencing electrophoretograms for the *EGFR* mutant cell lines positive for *EGFR* amplification also revealed that the mutant signals were dominant, and the wild-type sequence was barely detectable (Fig. 1), indicative of selective amplification of the mutant alleles. We used the recently proposed definition of *EGFR* amplification as determined by FISH (25, 27) and found that the pattern of gene amplification seemed to be dependent on the

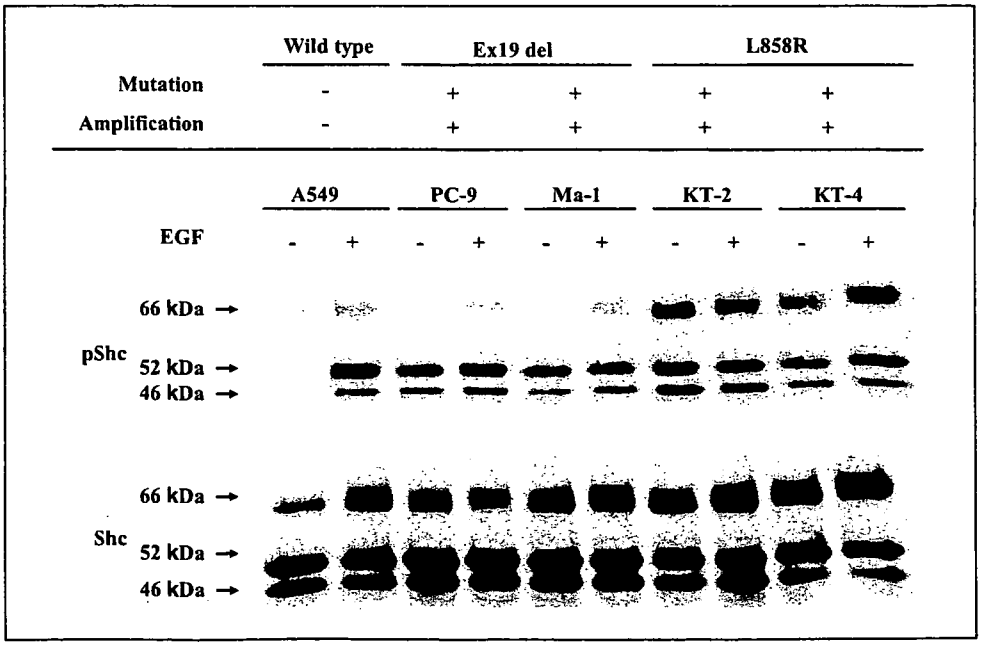

Figure 5. Phosphorylation of Shc in NSCLC cell lines. Serum-deprived cells were incubated for 15 min in the absence or presence of EGF (100 ng/mL), after which cell lysates (40 μg of protein) were subjected to immunoblot analysis with antibodies to phosphorylated Shc (*pShc*) or total Shc. Representative of three independent experiments.

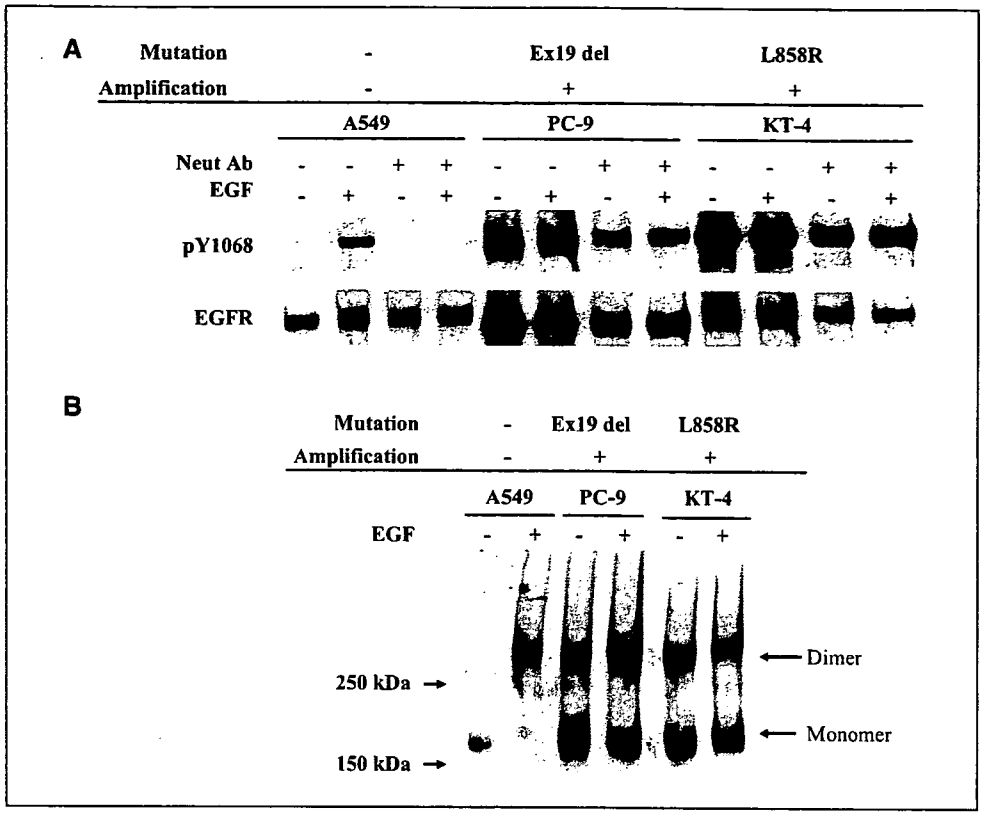

Figure 6. Mechanism of constitutive activation of EGFR in NSCLC cell lines. *A*, effect of neutralizing antibodies (*Neut Ab*) on EGFR phosphorylation. Serum-deprived NSCLC cells (A549, PC-9, or KT-4) were incubated for 3 h with a combination of neutralizing antibodies to EGF, TGF-α, and EGFR and then for 15 min in the additional absence or presence of EGF (100 ng/mL). Cell lysates were then prepared and subjected to immunoblot analysis with antibodies to the Y1068-phosphorylated form of EGFR or to total EGFR. *B*, EGFR dimerization. Serum-deprived cells were incubated for 15 min in the absence or presence of EGF (100 ng/mL), exposed to a chemical cross-linker, lysed, and subjected to immunoblot analysis with antibodies to EGFR. Representative of three independent experiments.

type of *EGFR* mutation; gene clusters were observed in cells with the L858R mutation in exon 21, whereas an *EGFR*/chromosome copy number ratio of ≥2 was detected in those with the small deletion [del(E746-A750)] in exon 19. Together, these data support the notion that *EGFR* mutation and amplification may be co-selected for during the growth of NSCLC cells. The four cell lines (PC-9, Ma-1, KT-2, and KT-4) positive for both *EGFR* mutation and amplification were sensitive to gefitinib, suggesting that *EGFR* amplification may increase sensitivity to gefitinib in *EGFR* mutant cells.

Previous biochemical studies of cells transiently transfected with vectors for wild-type or mutant forms of EGFR suggested that *EGFR* mutations increase EGF-dependent receptor activation (15, 30). Infection of NIH 3T3 cells with a retrovirus encoding *EGFR* mutants showed that the mutant receptors are constitutively activated and able to induce cell transformation in the absence of exogenous EGF (32). We examined the activation status of endogenous EGFRs in the six NSCLC cell lines that harbor *EGFR* mutations. The H1650, PC-9, and Ma-1 cell lines, all of which harbor the same exon 19 deletion, showed different patterns of EGFR autophosphorylation in the COOH-terminal region of the protein. EGFR autophosphorylation was ligand dependent in H1650 cells, which are negative for *EGFR* amplification, whereas Y1068 (but not Y845 and Y1173) was constitutively phosphorylated in PC-9 and Ma-1 cells, both of which manifest *EGFR* amplification. These results suggest that both *EGFR* mutation and amplification may be required for constitutive activation of EGFR in NSCLC cells that harbor the exon 19 deletion. In contrast, NSCLC cell lines (H1975, KT-2, and KT-4) that harbor the L858R mutation exhibited constitutive phosphorylation of EGFR at Y845, Y1068, and Y1173, regardless of the absence or presence of *EGFR* amplification. It is thought that *EGFR* mutations result in repositioning of critical residues surrounding the ATP-binding cleft of the tyrosine kinase domain of the receptor and thereby stabilize the interactions with ATP and EGF-TKIs, leading to increased tyrosine kinase activity and EGFR-TKI sensitivity (15, 23, 24). The differential activation of *EGFR* mutants observed in the present study may result from distinct conformational changes within the catalytic pocket caused by the different types of *EGFR* mutation. NSCLC patients with exon 19 deletions were recently shown to manifest longer overall survival than did those with the exon 21 point mutation after treatment with EGFR-TKIs, supporting the notion that the two major types of mutant receptors have different biological properties (46, 47).

Ligand-induced receptor dimerization underlies the activation of receptor tyrosine kinases (4, 5). Chemical cross-linking revealed that EGF binding to EGFR induced receptor dimerization in A549 cells, which express only the wild-type form of the receptor. In contrast, endogenous EGFRs in NSCLC cells harboring either the exon 19 deletion or the point mutation in exon 21 of *EGFR* were found to dimerize in the absence of ligand, suggesting that the constitutive activation of the mutant receptors is attributable to ligand-independent dimerization. EGFR dimerization was shown to be induced by interaction of quinazolines with the ATP-binding site of the receptor in the absence of ligand binding, suggesting that a change in conformation around the ATP-binding pocket of EGFR is sufficient for receptor dimerization (35). Conformational changes induced by *EGFR* mutations may therefore also trigger EGFR dimerization in *EGFR* mutant cells.

In conclusion, we have found that *EGFR* mutation is closely associated with *EGFR* amplification in NSCLC cell lines. Endogenous EGFRs expressed in NSCLC cells positive for both *EGFR* mutation and amplification are constitutively activated as a result

of ligand-independent dimerization. Cells with the two most common types of *EGFR* mutation also manifest different patterns of EGFR autophosphorylation. Prospective studies are required to determine the potential for exploitation of these *EGFR* alterations in the treatment of advanced NSCLC.

Acknowledgments

Received 9/12/2006; revised 10/30/2006; accepted 12/10/2006.

The costs of publication of this article were defrayed in part by the payment of page charges. This article must therefore be hereby marked *advertisement* in accordance with 18 U.S.C. Section 1734 solely to indicate this fact.

We thank Takeko Wada, Erina Hatashita, and Yuki Yamada for technical assistance.

References

1. Wang Y, Minoshima S, Shimizu N. Precise mapping of the EGF receptor gene on the human chromosome 7p12 using an improved FISH technique. Jpn J Hum Genet 1993;38:399–406.
2. Jorissen RN, Walker F, Pouliot N, Garrett TP, Ward CW, Burgess AW. Epidermal growth factor receptor: mechanisms of activation and signalling. Exp Cell Res 2003; 284:31–53.
3. Hynes NE, Lane HA. ERBB receptors and cancer: the complexity of targeted inhibitors. Nat Rev Cancer 2005; 5:341–54.
4. Ogiso H, Ishitani R, Nureki O, et al. Crystal structure of the complex of human epidermal growth factor and receptor extracellular domains. Cell 2002;110:775–87.
5. Schlessinger J. Ligand-induced, receptor-mediated dimerization and activation of EGF receptor. Cell 2002;110:669–72.
6. Hirsch FR, Varella-Garcia M, Bunn PA, Jr., et al. Epidermal growth factor receptor in non-small-cell lung carcinomas: correlation between gene copy number and protein expression and impact on prognosis. J Clin Oncol 2003;21:3798–807.
7. Suzuki S, Dobashi Y, Sakurai H, Nishikawa K, Hanawa M, Ooi A. Protein overexpression and gene amplification of epidermal growth factor receptor in nonsmall cell lung carcinomas. An immunohistochemical and fluorescence *in situ* hybridization study. Cancer 2005;103: 1265–73.
8. Shepherd FA, Rodrigues Pereira J, Ciuleanu T, et al. Erlotinib in previously treated non-small-cell lung cancer. N Engl J Med 2005;353:123–32.
9. Thatcher N, Chang A, Parikh P, et al. Gefitinib plus best supportive care in previously treated patients with refractory advanced non-small-cell lung cancer: results from a randomised, placebo-controlled, multicentre study (Iressa Survival Evaluation in Lung Cancer). Lancet 2005;366:1527–37.
10. Fukuoka M, Yano S, Giaccone G, et al. Multi-institutional randomized phase II trial of gefitinib for previously treated patients with advanced non-small-cell lung cancer (the IDEAL 1 trial). J Clin Oncol 2003;21: 2237–46.
11. Kaneda H, Tamura K, Kurata T, Uejima H, Nakagawa K, Fukuoka M. Retrospective analysis of the predictive factors associated with the response and survival benefit of gefitinib in patients with advanced non-small-cell lung cancer. Lung Cancer 2004;46:247–54.
12. Takano T, Ohe Y, Kusumoto M, et al. Risk factors for interstitial lung disease and predictive factors for tumor response in patients with advanced non-small cell lung cancer treated with gefitinib. Lung Cancer 2004;45:93–104.
13. Tamura K, Fukuoka M. Gefitinib in non-small cell lung cancer. Expert Opin Pharmacother 2005;6:985–93.
14. Ando M, Okamoto I, Yamamoto N, et al. Predictive factors for interstitial lung disease, antitumor response, and survival in non-small-cell lung cancer patients treated with gefitinib. J Clin Oncol 2006;24:2549–56.
15. Lynch TJ, Bell DW, Sordella R, et al. Activating mutations in the epidermal growth factor receptor underlying responsiveness of non-small-cell lung cancer to gefitinib. N Engl J Med 2004;350:2129–39.
16. Paez JG, Janne PA, Lee JC, et al. EGFR mutations in lung cancer: correlation with clinical response to gefitinib therapy. Science 2004;304:1497–500.
17. Pao W, Miller V, Zakowski M, et al. EGF receptor gene mutations are common in lung cancers from "never smokers" and are associated with sensitivity of tumors to gefitinib and erlotinib. Proc Natl Acad Sci U S A 2004; 101:13306–11.
18. Kosaka T, Yatabe Y, Endoh H, Kuwano H, Takahashi T, Mitsudomi T. Mutations of the epidermal growth factor receptor gene in lung cancer: biological and clinical implications. Cancer Res 2004; 64:8919–23.
19. Han SW, Kim TY, Hwang PG, et al. Predictive and prognostic impact of epidermal growth factor receptor mutation in non-small-cell lung cancer patients treated with gefitinib. J Clin Oncol 2005;23:2493–501.
20. Mitsudomi T, Kosaka T, Endoh H, et al. Mutations of the epidermal growth factor receptor gene predict prolonged survival after gefitinib treatment in patients with non-small-cell lung cancer with postoperative recurrence. J Clin Oncol 2005;23:2513–20.
21. Tokumo M, Toyooka S, Kiura K, et al. The relationship between epidermal growth factor receptor mutations and clinicopathologic features in non-small cell lung cancers. Clin Cancer Res 2005;11:1167–73.
22. Takano T, Ohe Y, Sakamoto H, et al. Epidermal growth factor receptor gene mutations and increased copy numbers predict gefitinib sensitivity in patients with recurrent non-small-cell lung cancer. J Clin Oncol 2005;23:6829–37.
23. Gazdar AF, Shigematsu H, Herz J, Minna JD. Mutations and addiction to EGFR: the Achilles 'heal' of lung cancers? Trends Mol Med 2004;10:481–6.
24. Shigematsu H, Gazdar AF. Somatic mutations of epidermal growth factor receptor signaling pathway in lung cancers. Int J Cancer 2006;118:257–62.
25. Cappuzzo F, Hirsch FR, Rossi E, et al. Epidermal growth factor receptor gene and protein and gefitinib sensitivity in non-small-cell lung cancer. J Natl Cancer Inst 2005;97:643–55.
26. Hirsch FR, Varella-Garcia M, McCoy J, et al. Increased epidermal growth factor receptor gene copy number detected by fluorescence *in situ* hybridization associates with increased sensitivity to gefitinib in patients with bronchioloalveolar carcinoma subtypes: a Southwest Oncology Group Study. J Clin Oncol 2005;23:6838–45.
27. Tsao MS, Sakurada A, Cutz JC, et al. Erlotinib in lung cancer: molecular and clinical predictors of outcome. N Engl J Med 2005;353:133–44.
28. Ishikawa N, Daigo Y, Takano A, et al. Increases of amphiregulin and transforming growth factor-α in serum as predictors of poor response to gefitinib among patients with advanced non-small cell lung cancers. Cancer Res 2005;65:9176–84.
29. Tracy S, Mukohara T, Hansen M, Meyerson M, Johnson BE, Janne PA. Gefitinib induces apoptosis in the EGFRL858R non-small-cell lung cancer cell line H3255. Cancer Res 2004;64:7241–4.
30. Sordella R, Bell DW, Haber DA, Settleman J. Gefitinib-sensitizing EGFR mutations in lung cancer activate anti-apoptotic pathways. Science 2004;305:1163–7.
31. Amann J, Kalyankrishna S, Massion PP, et al. Aberrant epidermal growth factor receptor signaling and enhanced sensitivity to EGFR inhibitors in lung cancer. Cancer Res 2005;65:226–35.
32. Greulich H, Chen TH, Feng W, et al. Oncogenic transformation by inhibitor-sensitive and -resistant EGFR mutants. PLoS Med 2005;2:1167–76.
33. Yonesaka K, Tamura K, Kurata T, et al. Small interfering RNA targeting survivin sensitizes lung cancer cell with mutant p53 to Adriamycin. Int J Cancer 2006; 118:812–20.
34. Koizumi F, Shimoyama T, Taguchi F, Saijo N, Nishio K. Establishment of a human non-small cell lung cancer cell line resistant to gefitinib. Int J Cancer 2005;116:36–44.
35. Arteaga CL, Ramsey TT, Shawver LK, Guyer CA. Unliganded epidermal growth factor receptor dimerization induced by direct interaction of quinazolines with the ATP binding site. J Biol Chem 1997;272:23247–54.
36. Mukohara T, Engelman JA, Hanna NH, et al. Differential effects of gefitinib and cetuximab on non-small-cell lung cancers bearing epidermal growth factor receptor mutations. J Natl Cancer Inst 2005;97:1185–94.
37. Janmaat ML, Rodriguez JA, Gallegos-Ruiz M, Kruyt FA, Giaccone G. Enhanced cytotoxicity induced by gefitinib and specific inhibitors of the Ras or phosphatidyl inositol-3 kinase pathways in non-small cell lung cancer cells. Int J Cancer 2006;118:209–14.
38. Pao W, Miller VA, Politi KA, et al. Acquired resistance of lung adenocarcinomas to gefitinib or erlotinib is associated with a second mutation in the EGFR kinase domain. PLoS Med 2005;2:225–35.
39. Kobayashi S, Ji H, Yuza Y, et al. An alternative inhibitor overcomes resistance caused by a mutation of the epidermal growth factor receptor. Cancer Res 2005; 65:7096–101.
40. Olayioye MA, Neve RM, Lane HA, Hynes NE. The ErbB signaling network: receptor heterodimerization in development and cancer. EMBO J 2000;19:3159–67.
41. Okabayashi Y, Kid Y, Okutani T, Sugimoto Y, Sakaguchi K, Kasuga M. Tyrosines 1148 and 1173 of activated human epidermal growth factor receptors are binding sites of Shc in intact cells. J Biol Chem 1994;269: 18674–8.
42. Riemenschneider MJ, Bell DW, Haber DA, Louis DN. Pulmonary adenocarcinomas with mutant epidermal growth factor receptors. N Engl J Med 2005;352:1724–5.
43. Shigematsu H, Lin L, Takahashi T, et al. Clinical and biological features associated with epidermal growth factor receptor gene mutations in lung cancers. J Natl Cancer Inst 2005;97:339–46.
44. Calvo E, Baselga J. Ethnic differences in response to epidermal growth factor receptor tyrosine kinase inhibitors. J Clin Oncol 2006;24:2158–63.
45. Sugio K, Uramoto H, Ono K, et al. Mutations within the tyrosine kinase domain of EGFR gene specifically occur in lung adenocarcinoma patients with a low exposure of tobacco smoking. Br J Cancer 2006;94:896–903.
46. Riely GJ, Pao W, Pham D, et al. Clinical course of patients with non-small cell lung cancer and epidermal growth factor receptor exon 19 and exon 21 mutations treated with gefitinib or erlotinib. Clin Cancer Res 2006; 12:839–44.
47. Jackman DM, Yeap BY, Sequist LV, et al. Exon 19 deletion mutations of epidermal growth factor receptor are associated with prolonged survival in non-small cell lung cancer patients treated with gefitinib or erlotinib. Clin Cancer Res 2006;12:3908–14.

Available online at www.sciencedirect.com
ScienceDirect
Cancer Letters 248 (2007) 292–298
CANCER Letters
www.elsevier.com/locate/canlet

Down-regulation of survivin by ultraviolet C radiation is dependent on p53 and results in G_2–M arrest in A549 cells

Masato Ikeda [a], Isamu Okamoto [a,*], Kenji Tamura [b], Taroh Satoh [a], Kimio Yonesaka [a], Masahiro Fukuoka [a], Kazuhiko Nakagawa [a]

[a] *Department of Medical Oncology, Kinki University School of Medicine, 377-2 Ohno-higashi, Osaka-Sayama, Osaka 589-8511, Japan*
[b] *Department of Medical Oncology, Kinki University School of Medicine Nara Hospital, Nara, Japan*

Received 27 May 2006; received in revised form 5 July 2006; accepted 2 August 2006

Abstract

Deregulation of survivin expression is implicated in tumorigenesis. To examine the regulation of survivin expression in response to DNA damage, we exposed A549 human lung cancer cells to ultraviolet C (UVC) radiation, which induces DNA single-strand breakage. UVC irradiation induced G_2–M arrest that was accompanied by accumulation of p53 and subsequent down-regulation of survivin. Depletion of p53 by RNA interference prevented the UVC-induced down-regulation of survivin. Furthermore, depletion of survivin resulted in G_2–M arrest, suggesting that down-regulation of survivin by p53 contributes to the p53-dependent G_2–M checkpoint triggered by DNA damage.

Keywords: Survivin; p53; RNA interference; G_2–M arrest; Ultraviolet C

1. Introduction

Survivin, a member of the inhibitor of apoptosis (IAP) family of proteins, is thought to play an important role in regulation of both apoptosis and cell division [1,2]. It is present in only small amounts in terminally differentiated normal cells but is overexpressed in almost all types of human malignancy [3–8]. Such overexpression of survivin is associated with poor prognosis in affected individuals, an increased rate of tumor recurrence, and resistance to certain anticancer agents and radiation [9,10].

The expression of survivin is regulated in a cell cycle-dependent manner. The promoter of the survivin gene possesses features typical of genes that are expressed at G_2–M phase of the cell cycle. Indeed, survivin is most abundant in cells at G_2–M and associates with the mitotic spindle of dividing cells [2]. Survivin interacts with Aurora B and inner centromere protein (INCENP), and the complex of Aurora B–INCENP–survivin monitors the integrity of the mitotic spindle [11]. It has been suggested that survivin controls the elimination by apoptosis of cells with an improperly formed mitotic spindle [3,12]. Overexpression of survivin in cancer may overcome cell cycle checkpoints and thereby facilitate aberrant progression of

* Corresponding author. Tel.: +81 72 366 0221; fax: +81 72 360 5000.
E-mail address: okamoto@dotd.med.kindai.ac.jp (I. Okamoto).

0304-3835/$ - see front matter © 2006 Elsevier Ireland Ltd. All rights reserved.
doi:10.1016/j.canlet.2006.08.005

transformed cells through mitosis. Although deregulation of survivin expression is an important event in tumorigenesis, the molecular mechanisms of survivin regulation are not fully understood.

The tumor suppressor p53 blocks progression of cells through the cell cycle or induces apoptosis [13,14]. Following its induction in response to DNA damage, p53 up-regulates the expression of various genes that contribute to cell cycle arrest, DNA repair, or apoptosis. It also negatively regulates the expression of a separate set of genes [15–18]. The functional loss of wild-type p53 has been shown to be associated with up-regulation of survivin expression in human cancers [19–21]. We have previously shown that the amounts of survivin mRNA and protein in cell lines positive for wild-type p53 decreased markedly after induction of p53 by adriamycin, which causes DNA double-strand breakage [22]. However, no such down-regulation of survivin was apparent in cell lines with mutated or null p53 alleles. These observations have suggested that p53 negatively regulates the expression of survivin in response to DNA damage.

In the present study, we show that exposure of p53-positive A549 human lung cancer cells to ultraviolet C (UVC) radiation, which induces DNA single-strand breakage, resulted in down-regulation of survivin expression after the induction of p53. Depletion of p53 by RNA interference (RNAi) prevented this down-regulation of survivin in cells exposed to UVC. Furthermore, RNAi-mediated depletion of survivin resulted in growth arrest in G_2–M phase of the cell cycle. These findings suggest that negative regulation of survivin by p53 contributes to the p53-dependent G_2–M checkpoint.

2. Materials and methods

2.1. Cell culture and irradiation

A549 cells were provided by Tohoku University (Miyagi, Japan). The cells were cultured under a humidified atmosphere of 5% CO_2 at 37 °C in RPMI 1640 medium (Sigma, St. Louis, MO) supplemented with 10% fetal bovine serum. Each batch of cells was discarded after 20 generations, and new batches were obtained from frozen stocks. Cells were exposed to UVC (30 J/m^2) with a Hoefer UVC 500 Ultraviolet Crosslinker (Amersham Pharmacia Biotech, Piscataway, NJ).

2.2. Immunoblot analysis

Cells were harvested by exposure to trypsin–EDTA, washed with phosphate-buffered saline (PBS), and lysed in a solution containing 30 mM HEPES, 1% Triton X-100, 10% glycerol, 5 mM $MgCl_2$, 25 mM NaF, 1 mM EDTA, and 10 mM NaCl. Equal amounts of lysate protein were fractionated by SDS–polyacrylamide gel electrophoresis at 100 V for 80 min at room temperature. The separated proteins were transferred to a nitrocellulose membrane, which was then probed for 2 h at room temperature with various primary antibodies, including affinity-purified rabbit polyclonal anti-survivin (R&D Systems, Minneapolis, MN), mouse monoclonal anti-p53 (Santa Cruz Biotechnology, Santa Cruz, CA), and affinity-purified rabbit polyclonal anti-β-actin (Sigma–Aldrich, St. Louis, MO). Immune complexes were detected with horseradish peroxidase-conjugated goat antibodies to rabbit immunoglobulin G (Amersham Biosciences, Little Chalfont, UK) or sheep antibodies to mouse immunoglobulin G (Santa Cruz Biotechnology) and with a chemiluminescence detection system (Perkin-Elmer, Boston, MA).

2.3. Flow cytometry

Cells were harvested, washed with PBS, fixed with 70% methanol, washed again with PBS, and stained with propidium iodide (0.05 mg/ml) in a solution containing 0.1% Triton X-100, 0.1 mM EDTA, and RNase A (0.05 mg/ml). The stained cells ($\sim 1 \times 10^5$) were than analyzed for DNA content with a flow cytometer (FACScaliber; Becton–Dickinson).

2.4. RNAi

Small interfering RNA (siRNA) duplexes specific for survivin or p53 mRNAs were synthesized by Dharmacon Research (Lafayette, CO) with the use of 2′-ACE protection chemistry. The survivin siRNA corresponded to nucleotides 206–224 of the coding region (GenBank Accession No. NM001168), whereas the p53 siRNA corresponded to nucleotides 775–793 of the coding region. BLAST searches of the human genome database were performed to ensure that the siRNA sequences would not target other gene transcripts. Cells in the exponential phase of growth were plated at a density of 3×10^4 cells per well in 12-well culture plates, cultured for 24 h, and then transfected with siRNA (300 nM) with the use of Oligofectamine in OPTI-MEM (Invitrogen, Carlsbad, CA). Control cells were treated with a scrambled siRNA duplex (Dharmacon).

2.5. Statistical analysis

Data are presented as means ± SD and were analyzed by Student's two-tailed t test (Stat View; SAS Institute, Cary, NC). A p value of <0.05 was considered statistically significant.

3. Results

3.1. UVC radiation inhibits A549 cell proliferation and induces G_2–M arrest

To evaluate the effect of UVC on A549 cell proliferation, we counted the number of viable cells at various times after irradiation. UVC treatment resulted in a 70% reduction in the number of viable cells compared with that for untreated cells at 48 h and a 60% reduction at 72 h (Fig. 1A). Flow cytometric analysis of cell cycle distribution revealed that this inhibition of cell proliferation by UVC was accompanied by an approximately twofold increase in the proportion of cells in G_2–M at 24 h (25.8% versus 13.4%), at 48 h (17.1% versus 7.9%) and at 72 h (12.3% versus 6.1%) compared with untreated cells (Fig. 1B), whereas irradiation had no marked effect on the sub-G_1 (apoptotic) population. These data indicated that treatment of A549 cells with UVC results in growth arrest at the G_2–M phase of the cell cycle.

3.2. UVC exposure induces p53 up-regulation followed by survivin down-regulation

Given that p53 mediates cell cycle arrest at the G_2–M transition in response to DNA damage and that we recently showed that down-regulation of survivin expression follows the accumulation of p53 in cells subjected to DNA double-strand breakage [22], we next examined whether survivin and p53 are functionally linked in A549 cells treated with UVC, which induces DNA single-strand breakage. Immunoblot analysis revealed that the abundance of p53 was increased 6 h after UVC exposure, reached a peak at 24 h, and then gradually returned to basal levels by 72 h (Fig. 2). In contrast, the amount of survivin began to decline at 48 h and its down-regulation was more pronounced at 72 h.

To determine whether p53 negatively regulates survivin expression, we examined the effect of UVC radiation on the abundance of survivin in cells depleted of p53 by RNAi. In cells transfected with a control (scrambled) siRNA or in nontransfected cells, the abundance of p53 was increased at 18 h after UVC exposure and the amount of

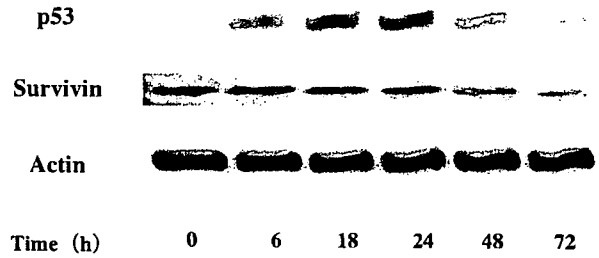

Fig. 2. Effects of UVC on the abundance of p53 and survivin in A549 cells. Total cellular protein extracted at the indicated times after exposure of cells to UVC (30 J/m^2) was subjected to immunoblot analysis with antibodies to p53, to survivin, or to β-actin (loading control). Data are representative of three independent experiments.

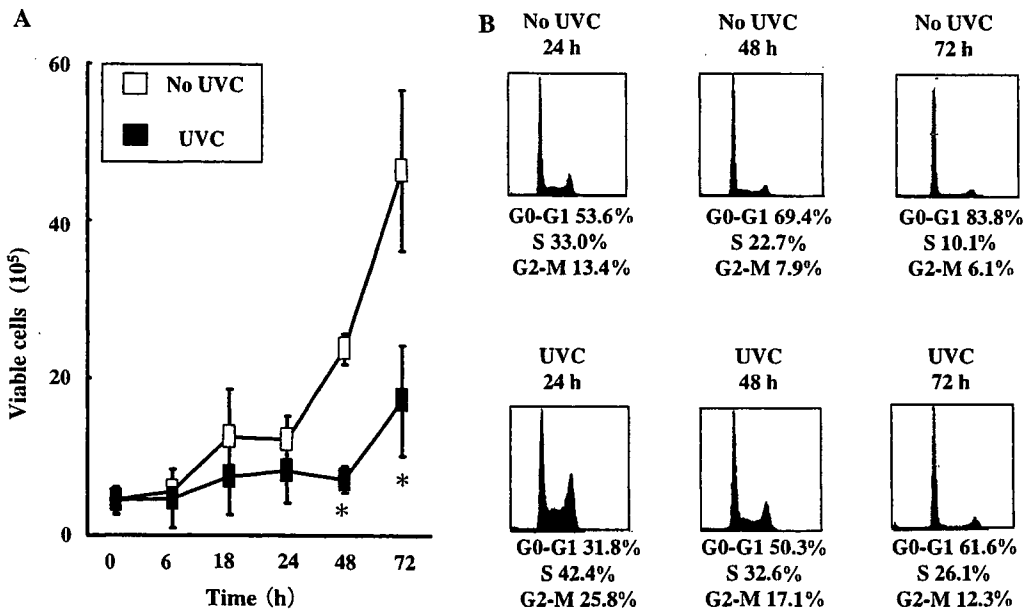

Fig. 1. Effects of UVC on the proliferation and cell cycle distribution of A549 cells. (A) Cell proliferation was evaluated by counting the number of viable cells by trypan blue staining at the indicated times after UVC irradiation (30 J/m^2). Data are means ± SD of values from three independent experiments. *$p < 0.05$ versus the corresponding value for cells not exposed to UVC. (B) Cell cycle distribution was analyzed by propidium iodide staining and flow cytometry at 24, 48 h and 72 h after UVC exposure. The percentages of cells at various stages of the cell cycle are indicated, and the data are representative of three independent experiments.

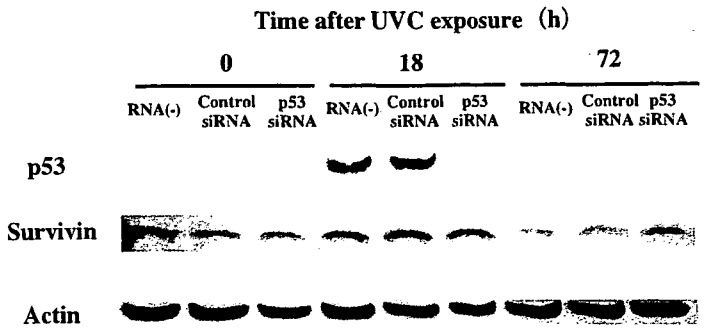

Fig. 3. Effect of UVC on the abundance of survivin in A549 cells depleted of p53 by RNAi. Cells were transfected (or not) with an siRNA specific for p53 mRNA or with a control (scrambled) siRNA, exposed to UVC (30 J/m^2), and subjected to immunoblot analysis with antibodies to p53, to survivin, or to β-actin at the indicated times after irradiation. Data are representative of three independent experiments.

survivin was decreased at 72 h (Fig. 3). In contrast, in cells transfected with an siRNA specific for p53 mRNA, UVC failed to increase p53 expression and had no effect on the level of survivin. These results thus indicated that induction of p53 by exposure of cells to UVC is necessary for down-regulation of survivin.

3.3. Ablation of survivin inhibits cell proliferation and induces G_2–M arrest

We next examined the effects of UVC irradiation in cells depleted of survivin by RNAi. The abundance of survivin was greatly reduced in cells transfected with an siRNA specific for survivin mRNA compared with that in nontransfected cells or cells transfected with a control (scrambled) siRNA (Fig. 4A). Cell proliferation (as evaluated from viable cell number) was also inhibited by 60% or 70% in cells subjected to transfection with the survivin siRNA for 48 or 72 h, respectively, compared with that apparent in nontransfected cells (Fig. 4B). The viable cell count was not affected by transfection with the control siRNA. Flow cytometry revealed that transfection of A549 cells with the survivin siRNA resulted in a marked increase in the proportion of cells in G_2–M at 48 and 72 h compared with that apparent for nontransfected cells or cells transfected with the control siRNA (Fig. 4C and D). There was no difference in the proportion of sub-G_1 cells among the three treatment groups.

4. Discussion

Several genes whose products play a role in control of the G_2–M transition of the cell cycle, including stathmin, Map4, cyclin B1, Cdc2, and Cdc25c, have been shown to be negatively regulated by p53 [15–18]. Repression of the expression of these genes in response to DNA damage requires wild-type p53 and contributes to a DNA damage-induced G_2–M checkpoint [23,24]. Survivin, a member of the IAP family of proteins, is maximally expressed at G_2–M and physically associates with microtubules of the mitotic spindle [2]. Previous studies have suggested that the expression of survivin is also subject to negative regulation by p53 [25–27], but the mechanism of such regulation has been unclear. We have now shown that exposure of the human lung cancer cell line A549 to UVC, which induces DNA single-strand breakage, resulted in the induction of endogenous p53 and a subsequent decrease in survivin expression. These observations are consistent with those of our previous study showing that survivin expression is repressed subsequent to p53 accumulation in cells treated with adriamycin [22], which induces DNA double-strand breakage. To investigate the possible role of p53 in the down-regulation of survivin induced by DNA damage, we depleted A549 cells of p53 by RNAi. Prevention of endogenous p53 accumulation in cells irradiated with UVC was found to block the repression of survivin expression, providing direct evidence that p53 is required for this effect of UVC. These data thus constitute further support for the notion that the survivin gene is a target of negative regulation by p53 in response to DNA damage.

The time course of survivin protein repression following UVC (DNA single-strand breakage)-induced p53 accumulation was almost identical to that observed in the cells having DNA double-strand breakage [22]. These results suggest that p53-dependent survivin suppression in response to these two types of DNA damage may share the common mechanisms at transcriptional level. Hoffmann et al. proposed that direct binding of p53 to a consensus binding site in the survivin gene promoter mediates transcriptional repression of the

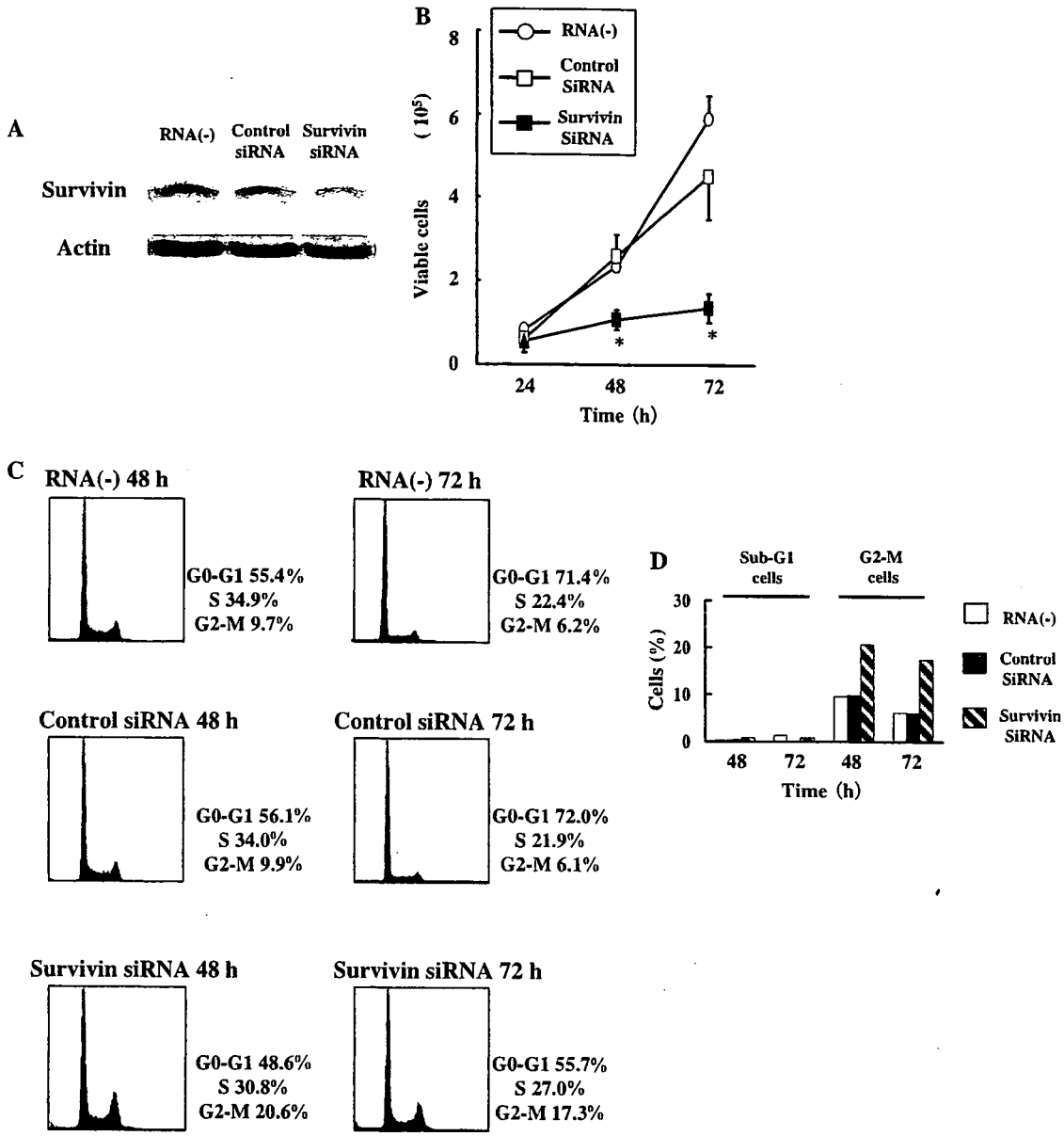

Fig. 4. Effects of survivin depletion by RNAi on the proliferation and cell cycle distribution of A549 cells. (A) Cells were transfected (or not) with a siRNA specific for survivin mRNA or with a control siRNA and were then subjected to immunoblot analysis with antibodies to survivin or to β-actin. Data are representative of three independent experiments. (B) Cells transfected for 24, 48, or 72 h as in (A) were evaluated for cell proliferation by counting the number of viable cells as revealed by staining with trypan blue. Data are means ± SD of values from three independent experiments. $*p < 0.05$ versus the corresponding value for nontransfected cells or cells transfected with the control siRNA. (C) The cell cycle distribution of cells transfected for 48 or 72 h as in (A) was determined by flow cytometry. The percentages of cells at various stages of the cell cycle are indicated. Data are representative of three independent experiments. (D) The percentages of sub-G_1 and G_2–M cells in the experiment shown in (C).

survivin gene by p53 [25]. In contrast, Mirza et al. suggested that chromatin deacetylation in the survivin promoter might contribute to p53-dependent repression of survivin gene expression in the absence of direct binding of p53 to the promoter DNA [26]. In the present study, repression of survivin expression was apparent 24 h after endogenous p53 accumulation, consistent with the results of our previous study [22]. This delay suggests that the mechanism of transcriptional inhibition of the survivin gene by p53 may be indirect. The repression of Cdc2 gene expression by p53 is mediated by a member of the E2F family of transcription factors subsequent to up-regulation of p21 and dephosphorylation of pRB family proteins [17]. However, UV-induced accumulation of p53 and subsequent

down-regulation of survivin have been observed in mouse embryonic fibroblasts derived from p21-null mice [29], suggesting that the ability of p53 to repress survivin gene expression is independent of its ability to up-regulate p21. The molecular mechanism by which p53 induces repression of survivin gene expression in response to DNA damage thus requires further investigation.

To examine the biological consequences of survivin gene repression in cells subjected to DNA damage, we depleted A549 cells of survivin by RNAi. Depletion of survivin resulted in growth arrest in G_2–M phase of the cell cycle, consistent with previous observations [28–31]. Survivin was originally proposed to perform an antiapoptotic function, but this issue remains controversial [29,32]. Indeed, several lines of evidence suggest that survivin plays an important role in regulation of mitotic events [11]. The chromosomal passenger complex (CPC), which consists of Aurora B, INCENP, and survivin, contributes to chromosome segregation and cytokinesis [33]. Depletion or inhibition of survivin or of the other proteins of the CPC thus results in mitotic arrest [30,34]. Furthermore, G_2–M arrest induced by survivin ablation was found to occur in $p53^{+/+}$ cells but not in $p53^{-/-}$ cells, implicating survivin in the p53-dependent G_2–M checkpoint that is essential for maintenance of genomic integrity [29]. Together, these various observations suggest that p53-induced repression of survivin expression in response to DNA damage may lower the threshold for apoptosis in cells in which the p53-dependent G_2–M checkpoint has been activated. Survivin repression following DNA damage may play critical role in deciding if lethal damaged cells die before DNA repair is completed, or if they will have the opportunity to repair and survive. Further characterization of the regulation of survivin in response to DNA damage may provide the basis for potential new approaches to cancer treatment that couple standard cytotoxic DNA-damaging agents with survivin-targeted therapy.

Acknowledgement

We thank Erina Hatashita and Yuki Yamada for technical assistance.

References

[1] G. Ambrosini, C. Adida, D.C. Altieri, A novel anti-apoptosis gene, survivin, expressed in cancer and lymphoma, Nat. Med. 3 (1997) 917–921.

[2] F. Li, D.C. Altieri, Transcriptional analysis of human survivin gene expression, Biochem. J. 344 (1999) 305–311.

[3] F. Li, E.J. Ackermann, C.F. Bennett, A.L. Rothermel, J. Plescia, S. Tognin, A. Villa, P.C. Marchisio, D.C. Altieri, Pleiotropic cell-division defects and apoptosis induced by interference with survivin function, Nat. Cell Biol. 1 (1999) 461–466.

[4] M. Monzo, R. Rosell, E. Felip, J. Astudillo, J.J. Sanchez, J. Maestre, C. Martin, A. Font, A. Barnadas, A. Abad, A novel anti-apoptosis gene: re-expression of survivin messenger RNA as a prognosis marker in non-small-cell lung cancers, J. Clin. Oncol. 17 (1999) 2100–2104.

[5] C. Adida, D. Berrebi, M. Peuchmaur, M. Reyes-Mugica, D.C. Altieri, Anti-apoptosis gene, survivin, and prognosis of neuroblastoma, Lancet 351 (1998) 882–883.

[6] A. Islam, H. Kageyama, N. Takada, T. Kawamoto, H. Takayasu, E. Isogai, M. Ohira, K. Hashizume, H. Kobayashi, Y. Kaneko, A. Nakagawara, High expression of Survivin, mapped to 17q25, is significantly associated with poor prognostic factors and promotes cell survival in human neuroblastoma, Oncogene 19 (2000) 617–623.

[7] H. Kawasaki, D.C. Altieri, C.D. Lu, M. Toyoda, T. Tenjo, N. Tanigawa, Inhibition of apoptosis by survivin predicts shorter survival rates in colorectal cancer, Cancer Res. 58 (1998) 5071–5074.

[8] H. Meng, C.D. Lu, Y.L. Sun, D.J. Dai, S.W. Lee, N. Tanigawa, Expression level of wild-type survivin in gastric cancer is an independent predictor of survival, World J. Gastroenterol. 10 (2004) 3245–3250.

[9] N. Zaffaroni, M.G. Daidone, Survivin expression and resistance to anticancer treatments: perspectives for new therapeutic interventions, Drug Resist. Update 5 (2002) 65–72.

[10] K. Asanuma, R. Moriai, T. Yajima, A. Yagihashi, M. Yamada, D. Kobayashi, N. Watanabe, Survivin as a radioresistance factor in pancreatic cancer, Jpn. J. Cancer Res. 91 (2000) 1204–1209.

[11] R. Honda, R. Korner, E.A. Nigg, Exploring the functional interactions between Aurora B, INCENP, and survivin in mitosis, Mol. Biol. Cell 14 (2003) 3325–3341.

[12] F. Li, G. Ambrosini, E.Y. Chu, J. Plescia, S. Tognin, P.C. Marchisio, D.C. Altieri, Control of apoptosis and mitotic spindle checkpoint by survivin, Nature 396 (1998) 580–584.

[13] R.V. Sionov, Y. Haupt, The cellular response to p53: the decision between life and death, Oncogene 18 (1999) 6145–6157.

[14] B. Vogelstein, D. Lane, A.J. Levine, Surfing the p53 network, Nature 408 (2000) 307–310.

[15] J. Ahn, M. Murphy, S. Kratowicz, A. Wang, A.J. Levine, D.L. George, Down-regulation of the stathmin/Op18 and FKBP25 genes following p53 induction, Oncogene 18 (1999) 5954–5958.

[16] S.A. Innocente, J.L. Abrahamson, J.P. Cogswell, J.M. Lee, p53 regulates a G2 checkpoint through cyclin B1, Proc. Natl. Acad. Sci. USA 96 (1999) 2147–2152.

[17] W.R. Taylor, A.H. Schonthal, J. Galante, G.R. Stark, p130/E2F4 binds to and represses the cdc2 promoter in response to p53, J. Biol. Chem. 276 (2001) 1998–2006.

[18] R. Zhao, K. Gish, M. Murphy, Y. Yin, D. Notterman, W.H. Hoffman, E. Tom, D.H. Mack, A.J. Levine, Analysis of p53-regulated gene expression patterns using oligonucleotide arrays, Genes Dev. 14 (2000) 981–993.